

Progress in the study of the (non)existence of genuinely unextendible product bases

Maciej Demianowicz¹

¹*Institute of Physics and Applied Computer Science, Faculty of Applied Physics and Mathematics,
Gdańsk University of Technology, Narutowicza 11/12, 80-233 Gdańsk, Poland*^{*}

(Dated: October 13, 2025)

We investigate the open problem of the existence of genuinely unextendible product bases (GUPBs), that is, multipartite unextendible product bases (UPBs) which remain unextendible even with respect to biproduct vectors across all bipartitions of the parties. To this end, we exploit the well-known connection between UPBs and graph theory through orthogonality graphs and orthogonal representations, together with recent progress in this framework, and employ forbidden induced subgraph characterizations to single out the admissible local orthogonality graphs for GUPBs. Using this approach, we establish that GUPBs of size thirteen in three-qutrit systems—the smallest candidate GUPBs—do not exist. We further provide a partial characterization of graphs relevant to larger bases and systems with ququart subsystems.

I. INTRODUCTION

Unextendible product bases (UPBs) [1, 2] constitute a very important notion in quantum information science, being relevant in a plethora of theoretical and practical areas. Specifically, one of the main results from the theory of entanglement related to UPBs is that a state supported on the orthogonal subspace is entangled and has positive partial transpose (PPT), i.e., it is PPT bound entangled [3]. UPBs also display the effect of nonlocality without entanglement [4–8]. Interestingly, UPBs found applications in the domain of Bell nonlocality, where they were exploited in the construction of Bell-type inequalities with no quantum violation [9, 10].

Much effort has been devoted to the characterization of UPBs, including establishing bounds on their sizes (see, e.g., [11–13]) and developing explicit constructions (see, e.g., [14–16]). In particular, the construction of UPBs with specific uncompleteness [17, 18] or unextendibility [19–21] properties has attracted considerable attention in the community. Despite this progress, a certain class of UPBs has remained elusive—genuinely unextendible product bases (GUPBs), i.e., UPBs which are unextendible in the strongest possible sense, that is even with biproduct vectors [20, 22]. In fact, while it has been shown that one can lower-bound the cardinalities of GUPBs in a non-trivial way, i.e., provide bounds which beat the ones stemming only from the theory of bipartite UPBs [22, 23], their actual existence, even in simple systems, remains an important open problem.

It was early recognized that UPBs share deep connections to combinatorial mathematics and graph theory [2, 24, 25]. Specifically, the notions of an orthogonality graph and an orthogonal representation of a graph prove very useful. Very recently, several strong general results in this framework were shown by Shi et al. in [23]. Their concise graph-theoretic characterization of UPBs also pushed forward our understanding of GUPBs. One particularly appealing result is that for certain minimal GUPBs their orthogonality graphs corresponding to single-partite subsystems are regular. This strong property severely narrows the set of eligible orthogonality graphs in these cases. Together with the fact that valid orthogonal representations of these graphs must satisfy certain spanning (or, saturation) properties, this paved way to investigate the existence of GUPBs in an organized fashion. Indeed, Shi et al. [23] put forward a concrete route to search for minimal, size thirteen, GUPBs in tripartite systems with qutrit subsystems—the smallest systems in which such bases may in principle exist. The proposition was to consider all thirteen-vertex four-regular graphs and check whether they admit orthogonal representations complying with certain requirements on their spanning properties. The realization of this idea in [23], relying on an optimization procedure in the search for orthogonal representations applied to all graphs from the relevant class, however, proved inconclusive, leaving the GUPB existence problem unsolved.

In this paper, we introduce the method of forbidden induced subgraph characterization into the search for GUPBs. The idea is to identify a small set of graphs, possibly with only a few vertices, that lack orthogonal representations in a given dimension. The relevant graph family is then pruned by discarding all graphs that contain any of these as induced subgraphs. Only the remaining graphs must then be checked for the existence of an orthogonal representation. With this aim, it is often possible to exploit further the properties of some smaller graphs and extract efficiently relevant features of representations and decide on their validity for the considered task. We apply this approach

^{*} maciej.demianowicz@pg.edu.pl

to the case of minimal GUPBs in three-qutrit systems and find that only two candidate graphs admit orthogonal representations, but these turn out not to be valid, leading us to conclude that the sought-for GUPBs do not exist. While we were able to obtain this result without investing much computational effort, in general, for larger systems or basis sizes, the approach will still require it. We discuss these limitations and the applicability of the method to other cases, and provide some initial results in this regard.

The paper is organized as follows. In Sec. II we introduce the relevant notions and notation. Sec. III focuses on the analysis of minimal three-qutrit GUPBs and forms the core of the paper. In Secs. IIIA–IIIC we analyze in detail all candidate graphs and argue that only two of them admit faithful orthogonal representations, which, nevertheless, are shown not to be valid for GUPBs. The main result of the paper is presented in Sec. IIID. In Sec. IV we discuss how the proposed approach can be applied to other cases, in particular to systems with qutrit or ququart subsystems. Finally, we conclude in Sec. V.

II. PRELIMINARIES

Let $\mathcal{H}_A = \mathcal{H}_{A_1} \otimes \cdots \otimes \mathcal{H}_{A_N}$ with $\mathcal{H}_{A_i} = \mathbb{C}^d$, where $A = A_1 A_2 \dots A_N$ label subsystems. A state $|\psi\rangle_A \in \mathcal{H}_A$ is said to be product if it can be written as $|\psi\rangle_A = |\varphi_1\rangle_{A_1} \otimes |\varphi_2\rangle_{A_2} \otimes \cdots \otimes |\varphi_N\rangle_{A_N}$. If a state is not product it is called entangled. Product states belong to a wider class of biproduct vectors which can be written as $|\psi\rangle_A = |\varphi\rangle_S \otimes |\bar{\varphi}\rangle_{\bar{S}}$ for some bipartition $S|\bar{S}$ of the subsystems (S and \bar{S} are disjoint sets such that $S \cup \bar{S} = A$). A state which is not biproduct is called genuinely multipartite entangled (GME). Subspaces of multipartite Hilbert spaces whose all vectors are entangled are called completely entangled (CES) [26–31]; a special class of such subspaces is comprised of those composed only of GME states — one calls them genuinely entangled subspaces (GESs) [20, 32–36]. In what follows we will omit normalization factors in states.

A. (Genuinely) unextendible product bases

We now briefly recall the notions of unextendible product basis [1, 2] and genuinely unextendible product basis [20, 22].

Definition 1. *An unextendible product basis (UPB) is a set of product, mutually orthogonal vectors spanning a proper subspace of a given multipartite Hilbert space with the property that there does not exist a product vector orthogonal to all the elements of the set.*

An exemplary UPB in $\mathbb{C}^3 \otimes \mathbb{C}^3 \otimes \mathbb{C}^3$ is given by the following set of nineteen vectors [37]:

$$\begin{aligned} & |\varphi_i\rangle_{A_1} |0\rangle_{A_2} |\psi_j\rangle_{A_3}, |\varphi_i\rangle_{A_1} |\psi_j\rangle_{A_2} |2\rangle_{A_3}, |2\rangle_{A_1} |\varphi_i\rangle_{A_2} |\psi_j\rangle_{A_3}, \\ & |\psi_j\rangle_{A_1} |2\rangle_{A_2} |\varphi_i\rangle_{A_3}, |\psi_j\rangle_{A_1} |\varphi_i\rangle_{A_2} |0\rangle_{A_3}, |0\rangle_{A_1} |\psi_j\rangle_{A_2} |\varphi_i\rangle_{A_3}, |S\rangle_{A_1 A_2 A_3}, \end{aligned} \quad (1)$$

$(i, j) = (0, 1), (1, 0), (1, 1)$, where $|\varphi_p\rangle = |1\rangle + (-1)^p |2\rangle$, $|\psi_p\rangle = |0\rangle + (-1)^p |1\rangle$, and $|S\rangle = (|0\rangle + |1\rangle + |2\rangle)^{\otimes 3}$ (so-called stopper state).

It follows from Definition 1 that the orthocomplement of a subspace spanned by a UPB is a CES. One should bear in mind that the converse does not hold in general.

Our scope is on a particular class of UPBs.

Definition 2. *A genuinely unextendible product basis (GUPB) is a set of product, mutually orthogonal vectors spanning a proper subspace of a given multipartite Hilbert space with the property that there does not exist a biproduct vector orthogonal to all the elements of the set. In other words, a GUPB is a UPB for all bipartitions of the subsystems.*

It is evident that a GUPB defines a GES in the orthogonal subspace. An immediate realization is that GUPBs cannot exist in systems with a qubit subsystem since bipartite UPBs in systems $\mathbb{C}^2 \otimes \mathbb{C}^n$ do not exist [2]. Therefore, the smallest system one needs to consider is with $N = 3$ and $d = 3$.

While it is still an open question whether GUPBs exist at all, it has been recently shown that their sizes \mathfrak{G} must be bounded from below as follows [22, 23]:

$$\mathfrak{G}(d, N) \geq \frac{Nd^{N-1} - 1}{N - 1}. \quad (2)$$

In some cases this bound can be slightly refined [23]. Clearly, the RHS of Eq. (2) could involve the ceiling function, however, GUPBs saturating the lower bound in the current form share a certain important graph-theoretic feature (see Sec. IIC), which will serve as a basis for our considerations.

B. Graphs

We now move to a terse review of the relevant graph theory notions (see, e.g., [38]).

An undirected simple graph $G = (V, E)$ consists of a nonempty finite set V , whose elements are called vertices (or nodes), and a finite set E of different unordered pairs of elements of V , whose elements are called edges. Any graph in the current paper is an undirected and simple one with nonempty E . We say that two vertices v_1 and v_2 of a graph are adjacent if there is an edge connecting them, i.e., $\{v_1, v_2\} \in E$. In such case, v_1 is said to be a neighbor of v_2 and vice versa. The neighborhood $\mathcal{N}(v)$ of a given vertex v in a graph is the set of all its neighbors. The degree $\deg(v)$ of a vertex v in a graph is the size of its neighborhood, i.e., $\deg(v) = |\mathcal{N}(v)|$. A graph whose all vertices have the same degree is called regular. In particular, if this degree is r then the graph is called r -regular. An $(n - 1)$ -regular graph with n vertices is said to be complete. In such graphs, all vertices are adjacent. Regular graphs will be of our main interest.

An adjacency matrix of graph G , $\mathcal{A}(G)$, is the matrix whose (i, j) -th entry equals to 1 if $\{v_i, v_j\} \in E$ and 0 if $\{v_i, v_j\} \notin E$. All the diagonal elements of \mathcal{A} are equal to 0.

A clique of a graph is a subset of its vertices with the property that any two vertices are adjacent; oftentimes a clique is considered to be a graph itself and this is the approach we will employ. A k -clique, denoted henceforward by C_k , is a clique with k vertices. The clique number $\omega(G)$ of a graph G is given by the number of vertices in a maximum clique of the graph.

Two vertices v_1 and v_2 are said to be connected if there is a path ¹ from v_1 to v_2 . A graph is connected if any two of its vertices are connected. Otherwise, it is called disconnected.

A closed path with at least one edge is called a cycle. The length of a shortest cycle in a graph is called its girth, denoted g .

A subgraph of G is any graph, whose all vertices belong to V and all edges belong to E . Given two graphs, $G_1 = (V_1, E_1)$ and $G_2 = (V_2, E_2)$, their union is the graph $G_1 \cup G_2 = (V_1 \cup V_2, E_1 \cup E_2)$. A decomposition of a graph $G = (V, E)$ is a set of its subgraphs $\{G_i = (V_i, E_i)\}_{i=1}^m$ such that $\bigcup_{i=1}^m G_i = G$. The disjoint union of graphs will be denoted as $G_1 + G_2$.

Let $W \subseteq V$ and $E_W \subseteq E$ be the subset of all edges in G with both endpoints in W . Then, $G[W] = (W, E_W)$ is called an induced subgraph of G . In an induced subgraph isomorphism problem, one is given two graphs G and H and must determine whether there exists an induced subgraph of G that is isomorphic to H . In full generality, it is an NP-complete problem.

1. Orthogonal representations and orthogonality graphs

An orthogonal representation (OR) in dimension d of a graph $G = (V, E)$ assigns vectors $|v_i\rangle \in \mathbb{C}^d$ to all vertices $v_i \in V$ in such a manner that $\langle v_i | v_j \rangle = 0$ for adjacent vertices. The representation is said to be faithful if the vectors are orthogonal only for adjacent vertices. In fact, we will be exclusively interested in the existence of faithful ORs for certain graphs. We will use $\text{FOR}(d)$ to denote a faithful OR in dimension d of a graph. An important problem in the field is finding the minimal dimension d_{\min} for which an orthogonal representation for a given graph exists. While it is in general very hard to find d_{\min} [39, 40], a simple useful lower bound is $d_{\min} \geq \omega(G)$.

Somewhat conversely, given a set of vectors $\{|\varphi_i\rangle\}_{i=1}^k$ from \mathbb{C}^d , their orthogonality graph (OG) is the graph $G = (V, E)$ with $V = \{v_1, v_2, \dots, v_k\}$ and $E = \{\{v_i, v_j\} : \langle \varphi_i | \varphi_j \rangle = 0\}$.

Notice that we consider here the notion of an orthogonal representation commonly used in quantum information theory, rather than the one introduced by Lovász [41] and widely spread throughout the mathematical literature, whereby the orthogonality of vectors is imposed for non-adjacent vertices (usually as an iff condition). The relation between these two approaches is evident: given graph G , the Lovász-type representation of the complement of G is the one we are interested in the present paper.

2. Forbidden induced subgraph characterization

In a forbidden graph characterization (see, e.g., [42–44]) one specifies completely a family of graphs through a set of subgraphs (or, more generally, substructures), called an obstruction set, such that none of the graphs from the

¹ A walk in graph $G = (V, E)$ is given by a (finite) sequence of edges $\{v_0, v_1\}, \{v_1, v_2\}, \dots, \{v_{m-1}, v_m\}$ in which any two consecutive edges are either adjacent or the same. A walk gives a sequence of vertices $v_0 v_1 \dots v_{m-1} v_m$. A walk with $v_0 = v_m$ is said to be closed; otherwise, it is open. The number of edges in a walk is called its length. A walk with all edges distinct is called a trail. Further, if vertices v_1, \dots, v_{m-1} are different then the trail is called a (simple) path.

family admits a subgraph (or a relevant substructure) from the obstruction set. Our main tool will be a variant of this approach, namely a forbidden induced subgraph characterization of graphs admitting a FOR. It relies on the following simple, yet powerful observation.

Observation 1. *Let G be a graph without a $\text{FOR}(d)$. Then any graph H containing G as an induced subgraph does not admit a $\text{FOR}(d)$ either.*

For a given dimension, our aim will be to identify a set of small graphs without FORs and then use Observation 1.

3. Orthogonal representation of the square graph and the diamond graph

We will repeatedly use the following simple result characterizing (faithful) orthogonal representations of certain elementary graphs.

Lemma 1. *(i) The square graph has at least one repeating vector in a $\text{FOR}(3)$. (ii) The diamond graph has exactly one repeating vector in a $\text{FOR}(3)$.*

Proof. See Fig. 1 for the denotations.

(i) Let $|w_1\rangle = |0\rangle$ and $|w_2\rangle = |1\rangle$. It must then hold $|w_3\rangle = |0\rangle + \alpha|2\rangle$ and $|w_4\rangle = |1\rangle + \beta|2\rangle$, and these vectors must be orthogonal, implying that $\alpha\beta = 0$.

(ii) It is obvious that the orthogonal representation with $|w_1\rangle = |0\rangle$, $|w_2\rangle = |1\rangle$, $|w_3\rangle = |w_4\rangle = |2\rangle$, which is faithful, is unique up to a unitary in $d = 3$. \square

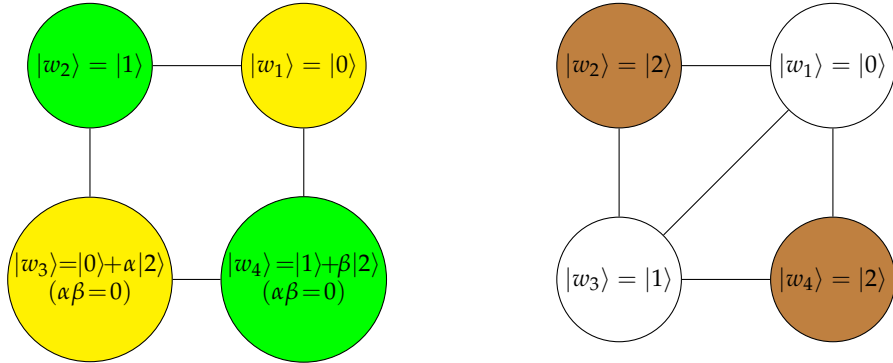


FIG. 1. (left) There is necessarily at least one repeating vector in a $\text{FOR}(3)$ of the square graph (Lemma 1) – for w_2 and w_4 (green) or w_1 and w_3 (yellow), or both. (right) There is necessarily exactly one pair of equal vectors, for w_2 and w_4 (brown), in a $\text{FOR}(3)$ of the diamond graph.

Notice that the square graph has in fact a pair of identical vectors in any OR in $d = 3$. Also, it is easy to observe that the necessary presence of repeated vectors does not hold for $d \geq 4$; we could, for example, set $|w_3\rangle = |0\rangle + |2\rangle + |3\rangle$ and $|w_4\rangle = |1\rangle + |2\rangle - |3\rangle$. Similarly for the diamond graph, where we could have $|w_2\rangle = |2\rangle$ and $|w_4\rangle = |2\rangle + |3\rangle$.

We will later use the square graph and the diamond graph to construct small graphs without FORs.

C. Graph-theoretic characterization of GUPBs

Let $\{|\varphi_1^{(j)}\rangle_{A_1} \otimes |\varphi_2^{(j)}\rangle_{A_2} \otimes \cdots \otimes |\varphi_N^{(j)}\rangle_{A_N}\}_{j=1}^k$, $|\varphi_i^{(j)}\rangle_{A_i} \in \mathbb{C}^d$, be a UPB. The number k is called the size or the cardinality of a UPB. One defines local orthogonality graphs (LOGs), G_i , $i = 1, 2, \dots, N$, for this set as follows: $G_i = (V, E_i)$, where $V = \{v_1, v_2, \dots, v_k\}$ and $E_i = \{\{v_m, v_n\} : \langle \varphi_i^{(m)} | \varphi_i^{(n)} \rangle_{A_i} = 0\}$. LOGs represent orthogonality of vectors in a UPB as seen by individual subsystems. Clearly, the union of LOGs G_i , which is an OG for the UPB, is a complete graph with k vertices, $\bigcup_{i=1}^N G_i = C_k$.

There is a simple necessary condition regarding spanning (saturation) properties of local vectors of a GUPB [22, 23].

Fact 1. *A k -element N -qudit GUPB must share the following property: for any subsystem A_m , any $(k - d^{N-1} + 1)$ -tuple of local vectors $|\varphi_m^{(j)}\rangle_{A_m}$ span the full d -dimensional subspace.*

A similar condition may also be formulated for the composed subsystems (containing up to $N - 1$ subsystems). All of them follow directly from the observation already made by Bennett et al. [1].

Further, we have the following result due to Shi et al. [23].

Fact 2. *LOGs for GUPBs saturating the lower bound in Eq. (2) are all $(\mathfrak{G} - d^{N-1})$ -regular.*

This powerful result places, in a sense, GUPBs on equal footing with UPBs, as a similar feature holds [23] for minimal UPBs of size $N(d - 1) + 1$ [1]. Furthermore, LOGs for those minimal GUPBs have non overlapping edge sets as can be realized through a direct count. Notably, a general result about the degrees of vertices in UPBs was also demonstrated in [23].

III. MINIMAL THREE-QUTRIT GUPBS

We now move the main part of the present paper and concentrate on the specific case of three-qutrit ($N = 3$ and $d = 3$) GUPBs. According to Eq. (2) their minimal permissible cardinality is (notice that this is also the smallest theoretically possible size of a GUPB in any setup)

$$\mathfrak{G}_{\min}(3, 3) = 13. \quad (3)$$

By Fact 2, LOGs for a minimal GUPB, which are now 13-vertex graphs, must be 4-regular. By Fact 1, for any subsystem A_m , any 5-tuple of local vectors $|\varphi_m^{(j)}\rangle_{A_m}$ in their FORs(3) span the full three-dimensional space. If a set of product vectors fulfills these conditions and in addition for any pair of subsystems $A_m A_n$, any 9-tuple of vectors $|\varphi_m^{(j)}\rangle_{A_m} \otimes |\varphi_n^{(j)}\rangle_{A_n}$ span the full 9-dimensional subspace then this set is a GUPB. This motivated Shi et al [23] to propose a concrete route for the search of minimal three-qutrit GUPBs. First, the complete graph C_{13} — representing an OG for a GUPB — needs to be decomposed into three 4-regular graphs, which play the role of LOGs. Second, one needs to find FORs for these LOGs sharing the single and two-partite spanning properties discussed above.

On the other hand, to disprove the existence of the minimal GUPBs it suffices to show that (a) certain candidate graphs do not have a FOR(3) and/or (b) FORs(3) for the remaining graphs do not lead to the fulfillment of the condition of Fact 1. We will follow this path. Observe that the ORs must necessarily be faithful as otherwise they would lead back to OGs which are not 4-regular anymore, contradicting Fact 2.

A. Candidate LOGs classification

We need to analyze all non-isomorphic 4-regular graphs with 13 vertices. Their total number is 10 786 [45] and they can be classified based on whether they are connected or not. More precisely, we can divide the graphs into:

- disconnected (Sec. III B) – 8 graphs [46],
- connected (Sec. III C) – 10 778 graphs [47].

The connected graphs will henceforth be denoted by M_i , where i is the index of a graph consistent with the enumeration obtained with GENREG software [48, 49]. A file with the adjacency matrices for these graphs is available at [50], where all other necessary resources can also be found.

We note that the connected graphs exhibit the following properties: (i) 31 graphs have girth 4 (precisely, graphs M_{10748} through M_{10778}) and (ii) the remaining graphs have girth 3 (they have 3-cliques, i.e., triangles, as subgraphs). The fact that there are no graphs with larger girths is what makes the square and the diamond graphs of particular relevance in our analyses.

B. Disconnected 4-regular graphs with 13 vertices

We begin with the simpler case of disconnected graphs. As noted in the previous section, there are 8 such graphs. They are of two types in terms of the number of vertices in the disconnected groups:

- (a) type I (6 graphs): $5 + 8$ vertices,
- (b) type II (2 graphs): $6 + 7$ vertices.

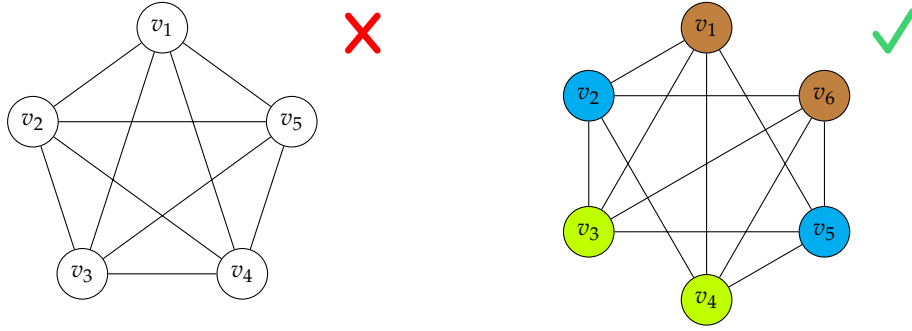


FIG. 2. (left) C_5 is the unique 4-regular graph on 5 vertices. Trivially, no FOR(3) exists for this graph (indicated by the cross mark). (right) The unique 4-regular graph D_6 on 6 vertices. This graph admits a FOR(3) (indicated by the checkmark) with necessarily repeating vectors for the colored vertices.

Let us analyze these graphs in detail.

(a) Type I. There are six 4-regular graphs with 8 vertices, however, there is only one such graph with 5 vertices, namely C_5 (Fig. 2), which obviously does not have a FOR(3). In turn, this case gets discarded.

(b) Type II. Graph D_6 (Fig. 2) is the unique graph with six vertices and there are two graphs with 7 vertices, $D_{7,a}$ and $D_{7,b}$ (Fig. 3).

Let us start with D_6 . Considering the diamond subgraph with vertices (v_1, v_2, v_3, v_4) immediately leads to $|v_3\rangle = |v_4\rangle$ (lime vertices in Fig. 2). In a similar manner we get $|v_2\rangle = |v_5\rangle$ (blue) and $|v_1\rangle = |v_6\rangle$ (brown). All three conditions can be satisfied simultaneously and we conclude that this graph does have a FOR(3) and it is unique up to a unitary.

We now consider $D_{7,a}$. Let $|v_1\rangle = |0\rangle$ and $|v_2\rangle = |1\rangle$. By Lemma 1, one immediately obtains $|v_3\rangle = |v_4\rangle = |v_5\rangle = |2\rangle$ (brown vertices in Fig. 3). Further, $|v_6\rangle = \alpha|0\rangle + \beta|1\rangle$, and $|v_7\rangle = \beta^*|0\rangle - \alpha^*|1\rangle$ with $\alpha, \beta \neq 0$. This constitutes a FOR(3), which is unique up to a unitary.

In case of $D_{7,b}$ there are several ways to arrive at a contradiction. For example, we readily get $|v_3\rangle = |v_4\rangle$, which is, however, impossible in a FOR as $\mathcal{N}(v_3) \neq \mathcal{N}(v_4)$. In turn, $D_{7,b}$ does not admit a FOR(3). In the framework of forbidden induced subgraph characterization (see Sec. III C), we identify $D_{7,b}$ as one admitting the forbidden subgraph H_5 (e.g., on vertices v_1, v_2, v_3, v_6, v_7).

Concluding, only one disconnected graph, $D_6 + D_{7,a}$ (type II), has a FOR(3). Nevertheless, this candidate graph gets discarded as there is twice the same vector in a FOR(3) for D_6 and thrice for $D_{7,a}$, violating the condition of Fact 1.

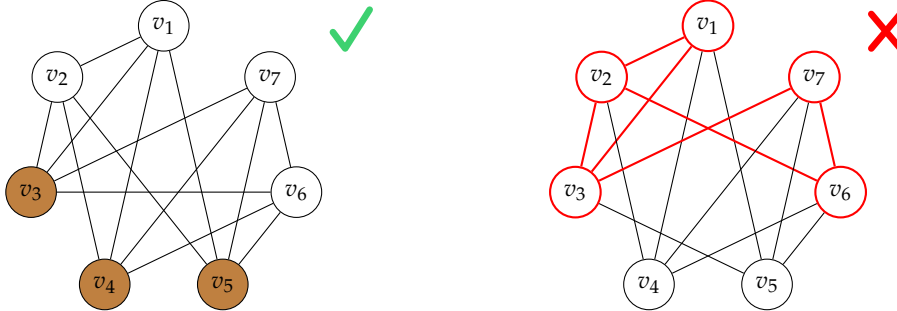


FIG. 3. Two non-isomorphic 4-regular graphs on 7 vertices: $D_{7,a}$ (left) and $D_{7,b}$ (right). $D_{7,a}$ admits a FOR(3) with the same vectors for v_3, v_4, v_5 ; there is no FOR(3) for $D_{7,b}$ as H_5 is its induced subgraph (highlighted in red).

For larger cases, there will be significantly more disconnected graphs (also with more vertices) and their analysis should involve the approach put forward in the next section.

C. Connected 4-regular graphs with 13 vertices

In this section we analyze all connected 4-regular graphs M_i , $i = 1, 2, \dots, 10\,778$ (cf. Sec. III A). With this purpose, we will use the approach of forbidden induced subgraph characterization (see Sec. II B 2). We will identify a small

number of graphs (with up to six vertices) not having a FOR(3) (an obstruction set). By Observation 1, if any of these graphs exists as an induced subgraph in graph M_i , then this graph obviously does not have a FOR(3) either and it gets discarded as a candidate LOG. We will be able to narrow the set of graphs having a FOR(3) down to a single graph. This graph will further be ruled out by Fact 1 as not having the required property.

Since the problem we deal here with is still rather small, we can employ a brute-force strategy for the relevant induced subgraph isomorphism problems. For a given subgraph, we verify whether its adjacency matrix \mathcal{A} or $P\mathcal{A}P^T$ (P is a permutation matrix) is a submatrix along the diagonal of the adjacency matrix of a graph from the analyzed set. This is performed for all subgraphs (see the list below) and all M_i 's. This is clearly very inefficient but it is particularly easy to implement and it is sufficient for the considered problem. We also implemented an alternative, more efficient procedure, using an in-built function for the subgraph isomorphism problem of the software we used [50].

1. Forbidden induced subgraphs

We will consider the following subgraphs:

- 4-clique C_4 (Fig. 4),
- house graph H_5 (Fig. 5),
- kite graph K_5 (Fig. 6),
- A -graph A_6 (Fig. 7).

Their adjacency matrices are as follows:

$$\mathcal{A}(C_4) = \begin{pmatrix} 0 & 1 & 1 & 1 \\ 1 & 0 & 1 & 1 \\ 1 & 1 & 0 & 1 \\ 1 & 1 & 1 & 0 \end{pmatrix}, \quad \mathcal{A}(H_5) = \begin{pmatrix} 0 & 1 & 1 & 1 & 0 \\ 1 & 0 & 1 & 0 & 1 \\ 1 & 1 & 0 & 0 & 0 \\ 1 & 0 & 0 & 0 & 1 \\ 0 & 1 & 0 & 1 & 0 \end{pmatrix}, \quad \mathcal{A}(K_5) = \begin{pmatrix} 0 & 1 & 1 & 1 & 0 \\ 1 & 0 & 1 & 1 & 0 \\ 1 & 1 & 0 & 0 & 1 \\ 1 & 1 & 0 & 0 & 0 \\ 1 & 1 & 0 & 0 & 0 \end{pmatrix}, \quad \mathcal{A}(A_6) = \begin{pmatrix} 0 & 0 & 0 & 1 & 1 & 1 \\ 0 & 0 & 0 & 0 & 1 & 1 \\ 0 & 0 & 0 & 0 & 0 & 1 \\ 1 & 0 & 0 & 0 & 0 & 0 \\ 1 & 1 & 0 & 0 & 0 & 0 \\ 1 & 1 & 1 & 0 & 0 & 0 \end{pmatrix}. \quad (4)$$

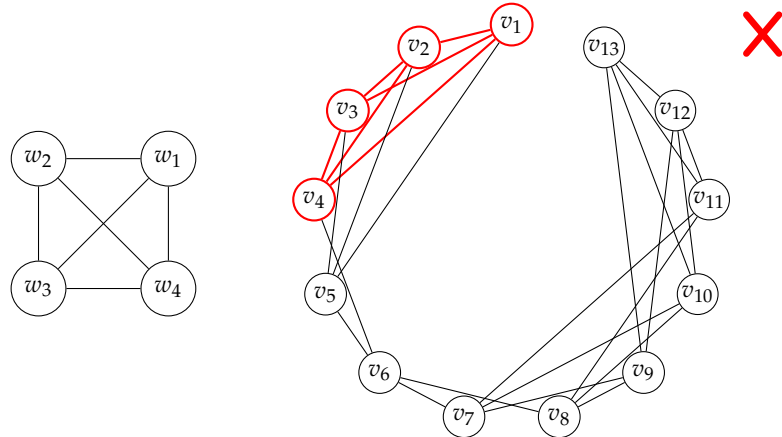


FIG. 4. (left) 4-clique C_4 . Graphs with 4-cliques obviously do not have FORs(3). (right) C_4 highlighted in red in M_4 .

Lemma 2. *Graphs: (a) C_4 , (b) H_5 , (c) K_5 , (d) A_6 do not admit a FOR(3).*

Proof. (a) Obvious. There is no orthogonal representation in $d \leq 3$ for this graph.

(b) By Lemma 1, it must be that $|w_2\rangle = |w_4\rangle$ or $|w_3\rangle = |w_5\rangle$. However, this is impossible to be achieved for a graph with $\mathcal{N}(w_2) \neq \mathcal{N}(w_4)$ and $\mathcal{N}(w_3) \neq \mathcal{N}(w_5)$ along with the condition that $|w_2\rangle \neq |w_5\rangle$ (there is edge $\{w_2, w_5\}$), which is the case here.

(c) It immediately follows that it must hold $|w_2\rangle = |w_4\rangle$ in any FOR(3). However, $\mathcal{N}(w_2) \neq \mathcal{N}(w_4)$, a contradiction.

(d) By Lemma 1 it must hold $|w_3\rangle = |w_5\rangle$ or $|w_2\rangle = |w_4\rangle$. However, it holds $\mathcal{N}(w_2) \neq \mathcal{N}(w_4)$ and $\mathcal{N}(w_3) \neq \mathcal{N}(w_5)$, preventing the graph to have a FOR(3). \square

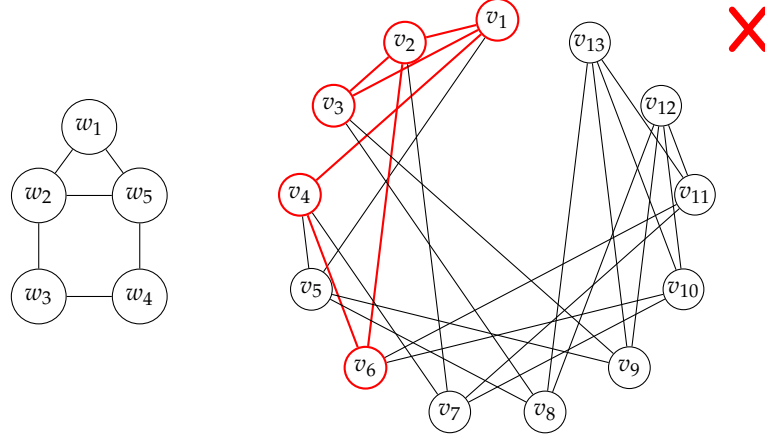


FIG. 5. (left) House graph H_5 — a 5-vertex graph without a FOR(3) [Lemma 2 (b)]. (right) H_5 highlighted in M_{9048} .

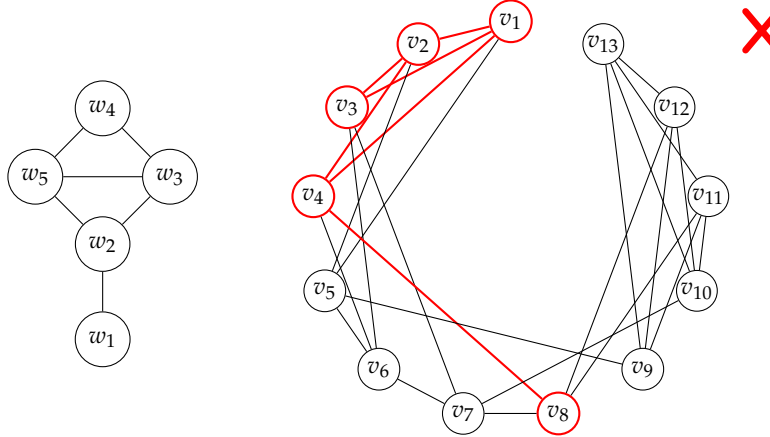


FIG. 6. (left) Kite graph K_5 — a 5-vertex graph without a FOR(3) [Lemma 2 (c)]. (right) K_5 highlighted in M_{503} .

We just note that it is a trivial task to find an OR in $d = 3$ for graphs A_6, K_5, H_5 .

Notably, C_4 is isomorphic to the wheel graph W_4 . Wheel graph W_n is given by an $(n - 1)$ -cycle with an extra vertex, called a hub, adjacent to all other vertices.

2. Forbidden induced subgraph characterization of graphs with FOR(3)

We define the following set

$$\mathcal{O}_3 = \{C_4, H_5, K_5, A_6\}. \quad (5)$$

We have verified through a direct automated search (see [50]) that \mathcal{O}_3 is an obstruction set for 13-vertex 4-regular graphs admitting a FOR(3). Interestingly, the latter family consists of a single graph — M_{5057} . In the next subsection we present a FOR(3) for this graph and argue that the graph cannot be a LOG for a minimal GUPB.

The results of the elimination procedure are shown in Tab. I and in more detail in Tab. III in Appendix D.

We have also verified that no three-element subset of \mathcal{O}_3 is enough to characterize the set of graphs with a FOR(3). It is possible that \mathcal{O}_3 is in fact minimal with regard to the considered task.

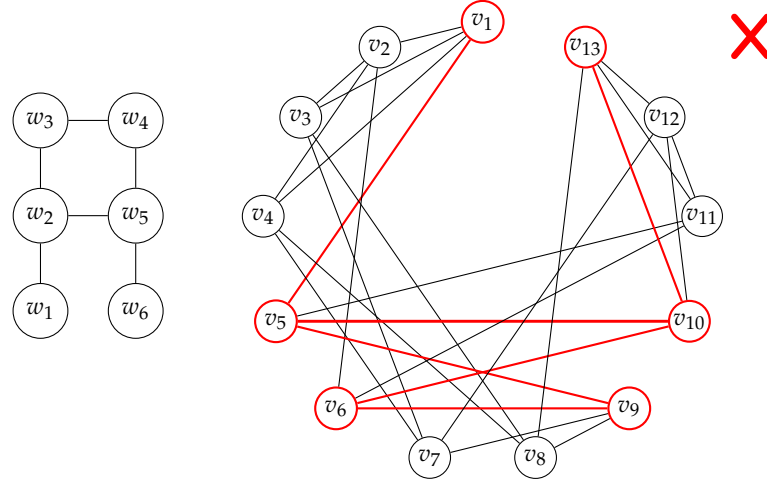


FIG. 7. (left) A-graph A_6 — a 6-vertex graph without a FOR(3) [Lemma 2 (d)]. (right) A_6 highlighted in graph M_{5059} .

13-vertex 4-regular connected graphs			
forbidden induced subgraph	# graphs w/ induced subgraph	cummulative # eliminated	# left
A-graph A_6	10 672	10 672	106
Kite graph K_5	8 919	10 767	11
House graph H_5	10 662	10 776	2
4-clique C_4	671	10 777	1

TABLE I. Summary of the forbidden induced subgraph characterization of 13-vertex 4-regular graphs with a FOR(3). Obstruction set \mathcal{O}_3 [Eq. (5)] defines a single graph.

3. FOR(3) for M_{5057}

Graph M_{5057} (see Fig. 8) has a FOR(3). An exemplary one is as follows:

$$\begin{aligned}
 |v_1\rangle &= |0\rangle, \quad |v_2\rangle = |1\rangle, \\
 |v_3\rangle &= |v_4\rangle = |2\rangle, \\
 |v_5\rangle &= 2|1\rangle - 3|2\rangle, \quad |v_6\rangle = 2|0\rangle - |2\rangle, \\
 |v_7\rangle &= |0\rangle - |1\rangle, \quad |v_8\rangle = |0\rangle + |1\rangle, \\
 |v_9\rangle &= |v_{10}\rangle = |v_{11}\rangle = |0\rangle + 3|1\rangle + 2|2\rangle, \\
 |v_{12}\rangle &= |0\rangle + |1\rangle - 2|2\rangle, \quad |v_{13}\rangle = |0\rangle - |1\rangle + |2\rangle.
 \end{aligned} \tag{6}$$

One immediately notices that this representation is not permissible according to Fact 1 because there is a 5-tuple of vectors whose span is only 2-dimensional, precisely:

$$\dim \text{span}\{|v_3\rangle, |v_4\rangle, |v_9\rangle, |v_{10}\rangle, |v_{11}\rangle\} = 2. \tag{7}$$

The FOR we gave above is not unique but the presence of repeating vectors leading to the above property is common to all representations of the graph.

Lemma 3. *In any FOR(3) of M_{5057} it holds: (a) $|v_3\rangle = |v_4\rangle$ and (b) $|v_9\rangle = |v_{10}\rangle = |v_{11}\rangle$.*

Proof. Case (a) is obvious as vertices v_3 and v_4 belong to the diamond graph with vertices (v_1, v_2, v_3, v_4) (highlighted in orange in Fig. 8).

For case (b), we need to consider (bipartite complete) subgraph with vertices $(v_5, v_6, v_9, v_{10}, v_{11})$ and edges $\{v_i, v_j\}$ with $i = 5, 6, j = 9, 10, 11$ (highlighted in bold in Fig. 8). We will now exploit Lemma 1 again. Consider the square graph with vertices $(v_5, v_{10}, v_6, v_{11})$ (blue in Fig. 8). It must be that (i) $|v_5\rangle = |v_6\rangle$ or (ii) $|v_{10}\rangle = |v_{11}\rangle$. Since $\mathcal{N}(v_5) \neq \mathcal{N}(v_6)$ in graph M_{5057} , case (i) can be discarded and case (ii) holds. Considering the square graph with (v_5, v_9, v_6, v_{11}) (thick, dashed) immediately leads then to $|v_9\rangle = |v_{11}\rangle$. Case (b) holds. As a note, observe that we could equivalently take v_{12} and v_{13} instead of v_5 and v_6 to arrive at the same conclusion. \square

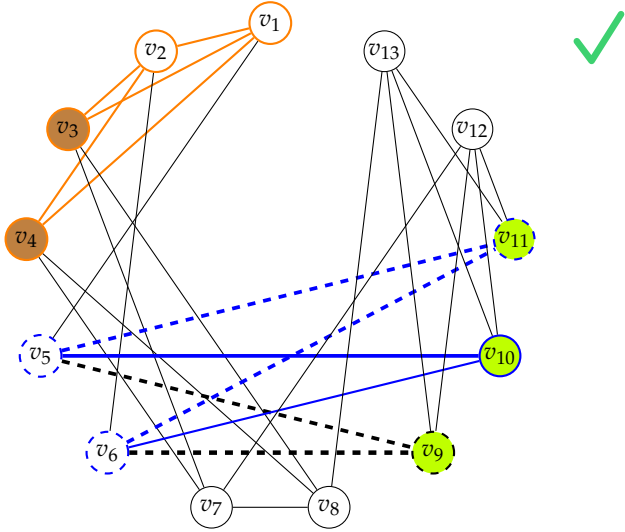


FIG. 8. Graph M_{5057} with the relevant subgraphs highlighted (see the proof of Lemma 3). There exist FORs(3) for this graph, e.g., the one given in Eq. (6); nevertheless, none of them complies with the requirement given in Fact 1 as the span of vectors corresponding to the colored vertices is always only 2-dimensional.

In consequence, candidate graph M_{5057} , while admitting FORs(3), gets discarded by Fact 1.

D. Thirteen element three-qutrit GUPB – conclusion

We have found that only two 4-regular graphs with 13 vertices have a faithful orthogonal representation in dimension three — $D_6 + D_{7,a}$ (disconnected) and M_{5057} (connected). However, none of them can be a LOG for a GUPB by Fact 1. This leads to the main result of the present paper.

Main result. *There does not exist a three-qutrit GUPB with a cardinality of 13.*

IV. GENERAL GUPBS

It is evident that the proposed method of forbidden induced subgraph characterization of graphs with a FOR is not fundamentally limited to the particular case of three-partite qutrit GUPBs of the so-far considered size. In principle, it can be applied universally for arbitrary N and d (or even different local dimensions for each subsystem; for clarity, we will omit these cases in further discussion) and cardinalities of the sets of vectors (not necessarily the minimal ones). The actual implementation in such cases, however, soon becomes intractable as the complexity of the problem grows very quickly (cf. Sec. IV B 2). In this section, we provide some initial results regarding the cases outside the one considered in Sec. III.

A. Qutrits

We can use set \mathcal{O}_3 to discard a number of candidate graphs (with $g = 3, 4$) in any case with $d = 3$. However, this set is not a universal obstruction set. For example, for 14-vertex 4-regular graphs (Sec. IV A 1 and Appendix B) we have identified an additional structure which should be included; it is relatively large as its vertex set has as many as eleven elements. On the other hand, we found that for some classes of 3-regular graphs (Sec. IV A 2 and Appendices C1-C2) the set can be reduced, which may also involve its modification.

1. 4-regular graphs with 14 vertices

We have performed an analysis analogous to the presented above in case of 14-vertex 4-regular graphs. One finds that there are 25 disconnected [46] and 88 186 connected [47] such graphs.

In case of disconnected graphs we now have three types: (a) type I (16 graphs): 5 + 9 vertices, (b) type II (6 graphs): 6 + 8 vertices, and (c) type III (3 graphs): 7 + 7 vertices.

We can use directly some of the results from Sec. III B. First, we can immediately discard type I graphs. Further, we find that there is a single type III graph with a FOR(3): $D_{7,a} + D_{7,a}$ (cf. Fig. 3). Finally, considering type II graphs, we recall that there is a unique 6-vertex 4-regular graph, D_6 , which does admit a FOR(3), so we need to check the 6 graphs $G_{8,i}$ with 8 vertices (see Fig. 9). We find that graphs $G_{8,1}$ through $G_{8,5}$ have an induced subgraph isomorphic to H_5 and as such do not admit FORs(3). It is trivial to realize that $G_{8,6}$ (which is a complete bipartite graph $K_{4,4}$) actually admits a FOR(2) as we can set $|v_2\rangle = |v_3\rangle = |v_4\rangle = |v_5\rangle = |0\rangle$ and $|v_1\rangle = |v_6\rangle = |v_7\rangle = |v_8\rangle = |1\rangle$. Clearly, this is not a unique (up to a unitary) FOR(3), however, it is easy to show that in any FOR(3) there will be four identical vectors (in Fig. 9, these will be vectors corresponding to green or yellow vertices). Consider vertex v_1 ; from $\mathcal{N}(v_1) = (v_2, v_3, v_4, v_5)$ we infer that $\mathfrak{d} := \dim \text{span}\{|v_2\rangle, |v_3\rangle, |v_4\rangle, |v_5\rangle\} \leq 2$. If $\mathfrak{d} = 2$, then it obviously holds $\dim \text{span}\{|v_1\rangle, |v_6\rangle, |v_7\rangle, |v_8\rangle\} = 1$ and the claim follows; if $\mathfrak{d} = 1$, the result trivially holds.

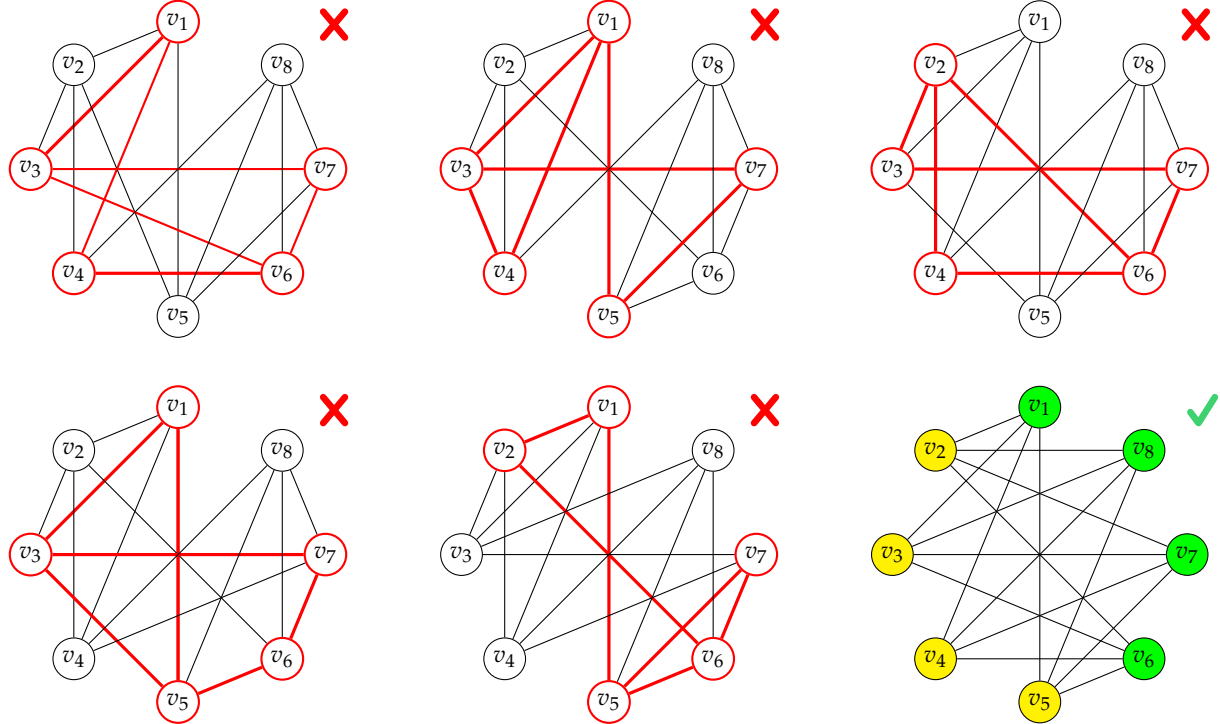


FIG. 9. All six 4-regular graphs with 8 vertices. Top row (from the left): $G_{8,1}$, $G_{8,2}$, $G_{8,3}$, bottom row (from the left): $G_{8,4}$, $G_{8,5}$, $G_{8,6}$. Induced subgraphs of $G_{8,i}$, $i = 1, 2, 3, 4, 5$, which are isomorphic to H_5 are highlighted in red; none of these graphs can have a FOR(3). $G_{8,6}$ does not have any of the graphs from \mathcal{O}_3 as an induced subgraph. This graph admits a FOR(3) with at least four identical vector; see the main text.

Let us now move to the connected graphs. We will denote these graphs by N_i with their enumeration in accordance with the GENREG output [49]. Among the connected graphs, we find that 220 graphs have $g = 4$ and the remaining

ones have $g = 3$. We can use set \mathcal{O}_3 from Eq. (5) for graph elimination, which leaves us only 7 graphs (depicted in Fig. 15 in Appendix B):

$$N_{2359}, N_{11743}, N_{36919}, N_{80015}, N_{87949}, N_{87956}, N_{87957}. \quad (8)$$

We analyze these graphs in Appendix B, where we find that only N_{80015} does not have a FOR(3). The induced subgraph \widehat{N}_{11} (see Fig. 16), which eliminates this graph is much larger than the elements of \mathcal{O}_3 as it has eleven vertices. We have the following obstruction set for the analyzed case (see Tab. II):

$$\widehat{\mathcal{O}}_3 = \mathcal{O}_3 \cup \{\widehat{N}_{11}\} = \{C_4, H_5, K_5, A_6, \widehat{N}_{11}\}. \quad (9)$$

2. Fourteen-element three-qutrit GUPBs - remarks

Let us now turn our attention to the case of 14-element three-qutrit GUPBs. Exploiting Fact 1, we can discard $D_{7,a} + D_{7,a}$ and $D_6 + D_{8,6}$ (disconnected) and N_{2359} and N_{87949} (connected) as LOGs in this case. At the same time, we have not been able to find an argument which could also eliminate the remaining connected graphs and thus their status is undecided.

It must be noted that 4-regular graphs are not sufficient in this case, i.e., not all LOGs must be of this type. This can be seen through a counting mismatch: each 4-regular graph on 14 vertices has 28 edges, so three such graphs could only account for thrice this number of edges, i.e., 84, while the complete graph C_{14} has 91 edges. However, by the same argument, decomposition of C_{14} into two 4-regular graphs and one 5-regular graph (with 35 edges) or one 3-regular graph (with 21 edges) and two 5-regular graphs is possible.

We find that there are 509 connected 3-regular graphs [51]. Among them there are 110 graphs with $g \geq 4, 9$ with $g \geq 5$, including one with $g = 6$; the remaining ones have $g = 3$ (there are no graphs with $g \geq 7$). Obstruction set \mathcal{O}_3 (in fact, set $\mathcal{O}_3 \setminus C_4$ as the connected 3-regular graphs do not contain 4-cliques) defines 57 graphs – 42 graphs with $g = 3$, six graphs with $g = 4$, and obviously the nine graphs with $g \geq 5$. We found that all the forty-eight graphs with $g = 3$ and $g = 4$ do have permissible FORs(3). This is also the case for the eight graphs with $g = 5$. We have not been able to show whether the single graph with $g = 6$ has a FOR(3). In Appendix C1, we gathered the relevant data.

There are also 31 disconnected 3-regular graphs [52]. These are of three types: (a) 4 + 10 vertices ($1 \times 19 = 19$ graphs), (b) 6 + 8 vertices ($2 \times 5 = 10$ graphs), (c) 4 + 4 + 6 (2 graphs). Types (a) and (c) get immediately eliminated as 3-regular graphs with four vertices are just 4-cliques. In Appendix C2, we provide a brief analysis of the graphs that remain after this initial elimination.

There are further 3 459 383 connected (seven graphs with $g = 4$ and the remaining ones with $g = 3$) and 3 disconnected 5-regular graphs (the disconnected ones get immediately discarded as they correspond to the division 6 + 8 of vertices; there are no 5-regular graphs with seven vertices) [53, 54]. We have not analyzed the connected graphs with our approach and leave it for future study.

In general, by the results of [23], we find that the degrees of vertices in LOGs are non-trivially bounded and belong to the set $\{3, 4, 5\}$. We do not know the number of non-isomorphic graphs of this type; we just note that there are $\binom{16}{2} = 120$ relevant degree sequences (including the three sequences of all 3s, 4s, or 5s). One also needs to bear in mind that the degrees of vertices of two-party orthogonality graphs comply with certain non-trivial conditions.

B. Ququarts

We now provide some partial results concerning bases with ququart subsystems ($d = 4$).

1. Small graphs without a FOR(4)

Our procedure exploits the fact that there are necessarily repeated vectors in FORs for certain smaller subgraphs (the non-existence of FORs for cliques can also be explained from this point of view). This allows for the elimination of candidate graphs but also proves useful in the characterization of FORs for the graphs possessing them. In case of qutrits, the elementary structures with the property are the square graph and the diamond graph (Lemma 1). In this subsection, we give some simple graphs not admitting FORs in dimension $d = 4$, priorly identifying graphs with repeating vectors in a FOR(4).

14-vertex 4-regular connected graphs

forbidden induced subgraph	# graphs w/ induced subgraph	cummulative # eliminated	# left
A-graph A_6	87 868	87 868	300
Kite graph K_5	71 322	88 139	29
House graph H_5	87 537	88 158	10
4-clique C_4	4 184	88 161	7
\hat{N}_{11} (Fig. 16)	33	88 162	6

TABLE II. Summary of the forbidden induced subgraph characterization of 14-vertex 4-regular graphs with a FOR(3). Obstruction set \mathcal{O}_3 defines seven graphs (first four rows of the table). One more graph gets eliminated by its forbidden induced subgraph \hat{N}_{11} leaving six graphs, which we show to have FORs(3).

We begin with a consideration of a wheel graph and graphs obtained from it: envelope graphs E_6 and E_6^\perp , and $W_7^{\parallel\parallel}$ (see Fig. 10). The derived graphs are direct analogs of the house graph H_5 and A-graph A_6 , respectively.

Lemma 4. (a) *Wheel graph W_4 has at least one repeated vector in a FOR(4).* (b) *Envelope graph E_6 and graph E_6^\perp do not have FORs(4).* (c) *Graph $W_7^{\parallel\parallel}$ does not admit a FOR(4).*

Proof. (a) W.l.o.g. we set $|w_1\rangle = |0\rangle$, $|w_2\rangle = |1\rangle$, and $|w_3\rangle = |2\rangle$. Then it must be $|w_4\rangle = |1\rangle + \alpha|3\rangle$ and $|w_5\rangle = |0\rangle + \beta|3\rangle$; these graphs are orthogonal implying $\alpha\beta = 0$.

(b, c) For the three graphs the argument is the same: neighborhoods of vertices with equal vectors are different, a contradiction. \square

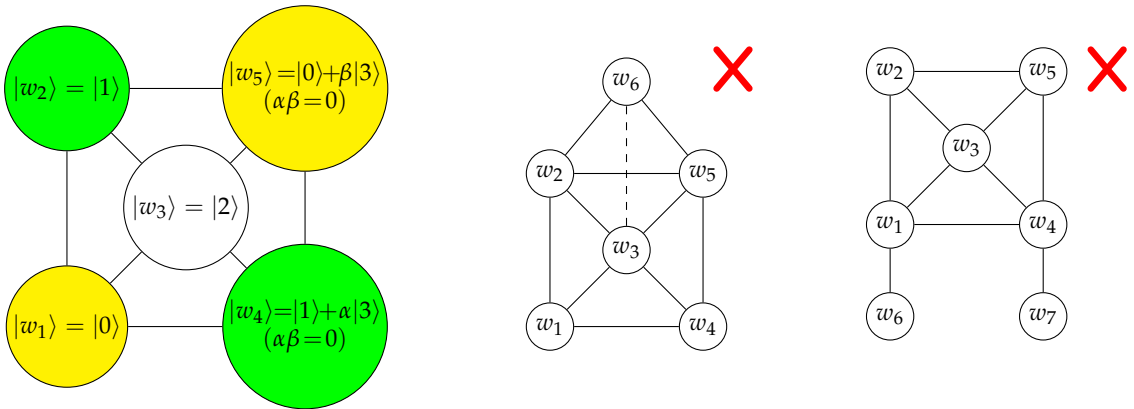


FIG. 10. (left) Wheel graph W_5 — an exemplary small graph with a necessarily repeated vector in a FOR(4) [Lemma 4 (a)]. (middle) Envelope graphs E_6 (solid edges only) and E_6^\perp (solid edges with additional dashed edge $\{w_3, w_6\}$) do not admit FORs(4) [Lemma 4 (b)]. (right) Graph $W_7^{\parallel\parallel}$ — a 7-vertex graph without a FOR(4) [Lemma 4 (c)].

We further have another graph leading to forbidden induced subgraphs (Fig. 11).

Lemma 5. (a) *Balloon graph B_5 has exactly one repeated vector in a FOR(4).* (b) *Graph B_6° does not admit a FOR(4).* (c) $C_4^{(3)}$ does admit a FOR(4).

Proof. Both assertions are rather trivial. (a) We can set $|w_1\rangle = |0\rangle$, $|w_2\rangle = |1\rangle$, $|w_3\rangle = |2\rangle$, $|w_4\rangle = |3\rangle$, as the corresponding graph is the clique C_4 . It immediately follows that $|w_5\rangle = |w_2\rangle = |1\rangle$. (b) Neighbors of vertices with the same vector in a FOR are different, a contradiction. (c) The graph is composed of three cliques C_4 , sharing certain vertices and edges (that is why the denotation for the graph). It follows that it must be $|w_2\rangle = |w_5\rangle$ and $|w_3\rangle = |w_6\rangle$, but w_5 and w_6 are not neighbors, while w_2 and w_3 are ones. \square

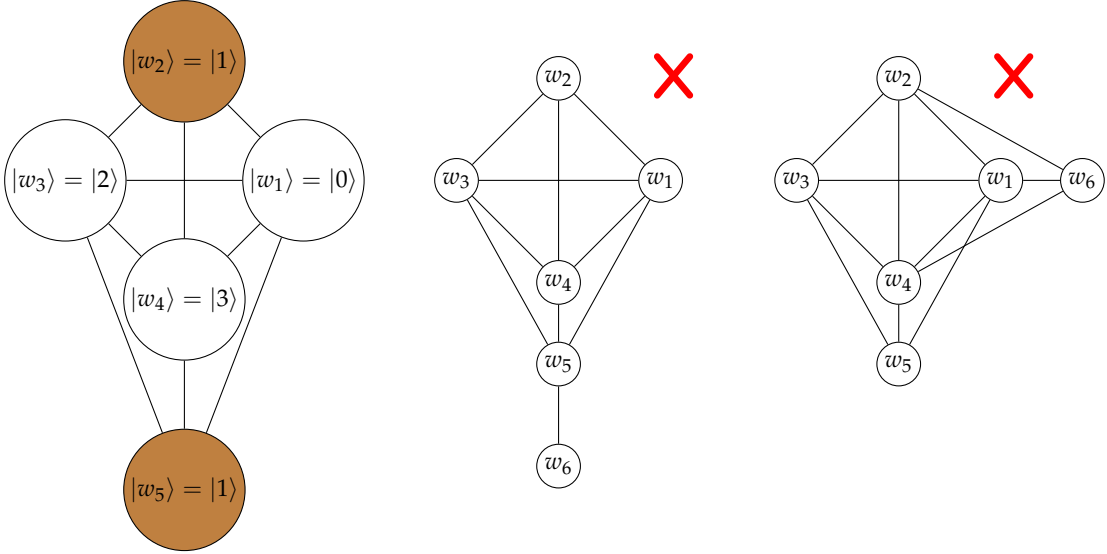


FIG. 11. (left) Balloon graph B_5 : there is one repeated vector in its FOR(4) [Lemma 5 (a)]. (middle) B_6^o – a 6-vertex graph without a FOR(4) [Lemma 5 (b)]. (right) Graph $C_4^{(3)}$ does not have a FOR(4) [Lemma 5 (c)].

2. Three-ququart minimal GUPBs - remarks

In the three-ququart case ($N = 3$, $d = 4$), it holds $\mathfrak{C}_{\min}(4,3) = 24$ and thus graphs with 24 vertices are the objects of interest. Importantly, the minimal GUPBs do not saturate the lower bound in Eq. (2) and we find that the degrees of vertices in LOGs are either 7 or 8 [23]. The number of valid degree sequences in this case is 25. Focusing only on relevant regular graphs, we find the following. They all have girth bounded as $g \leq 4$. There are 141 515 621 596 238 755 266 884 806 115 631 connected [55] and 733 460 349 818 disconnected [56] 7-regular graphs. We consider disconnected 8-regular, i.e., octic graphs more closely below.

There are 1 473 822 243 disconnected octic graphs on 24 vertices [57]. Their classification according to the division of vertices into two groups is as follows (dividing into more than two groups is impossible in this case):

- (a) type A: 9 + 15 vertices (1 470 293 676 graphs). These graphs get immediately discarded as there is the unique octic graph with 9 vertices — the clique C_9 ,
- (b) type B: 10 + 14 vertices (3 459 386 graphs). This case also gets discarded as there is one octic graph with 10 vertices and it contains C_5 as a subgraph (this can be verified by direct inspection or using Turán's bound [58]),
- (c) type C: 11 + 13 vertices ($6 \times 10\ 778 = 64\ 716$ graphs). There is only one graph among the six 11-vertex graphs, which does not contain C_5 , but it contains $C_4^{(3)}$ as an induced subgraph (see Fig. 12); consequently, type C graphs are eliminated,
- (d) type D: 12 + 12 vertices. There are 94 octic graphs on 12 vertices, giving rise to the total of 4 465 graphs. Among the said twelve-vertex octic graphs graphs we find 6 graphs with C_6 and 75 graphs with C_5 , which are eliminated at once (accounting for the total of 81 graphs). In turn, the remaining thirteen graphs give rise to 91 type D candidate graphs, which need to be checked for validity as LOGs. We have found that only two graphs, both shown in Fig. 13, do not get discarded by the induced forbidden subgraph $C_4^{(3)}$. Using again the enumeration of graphs from GENREG, these are graphs number 70 (with maximum clique C_4) and 94 (with

maximum clique C_3), denoted henceforth as L_{70} and L_{94} , respectively. We further find that E_6^\perp is an induced subgraph of L_{70} and this graph gets discarded. In turn, the only relevant graph from this category is $L_{94} + L_{94}$. We deal with L_{94} below.

Graph L_{94} is a complete 3-partite graph and as such it has a FOR even in dimension $d = 3$:

$$\begin{aligned} |v_1\rangle &= |v_{10}\rangle = |v_{11}\rangle = |v_{12}\rangle = |0\rangle, \\ |v_2\rangle &= |v_7\rangle = |v_8\rangle = |v_9\rangle = |1\rangle, \\ |v_3\rangle &= |v_4\rangle = |v_5\rangle = |v_6\rangle = |2\rangle. \end{aligned} \quad (10)$$

We will now show that even exploiting the extra dimension does not lead to a representation with appropriate spanning (saturation) properties. Let $\mathcal{A}_1 = \{|v_1\rangle, |v_{10}\rangle, |v_{11}\rangle, |v_{12}\rangle\}$, $\mathcal{A}_2 = \{|v_2\rangle, |v_7\rangle, |v_8\rangle, |v_9\rangle\}$, and $\mathcal{A}_3 = \{|v_3\rangle, |v_4\rangle, |v_5\rangle, |v_6\rangle\}$. While the obvious upper bound on the dimension of the subspaces spanned by the sets is three, we can immediately infer that it actually must hold that $\sum_k \dim \text{span} \mathcal{A}_k \leq 4$, as the division of vectors into three sets corresponds to a certain decomposition of the four dimensional Hilbert space, or its subspace, into orthogonal subspaces (the upper bound on the sum of dimensions is d in the general case of complete d -partite graphs). This means that there are always eight vectors in a representation that span only a two-dimensional subspace. Consequently, any FOR(4) of $L_{94} + L_{94}$ does not comprise with the condition imposed by Fact 1. An exemplary FOR(4) for L_{94} saturating dimensions of the subspaces spanned by the set is as follows:

$$\begin{aligned} |v_1\rangle &= |v_{10}\rangle = |v_{11}\rangle = |v_{12}\rangle = |0\rangle, \\ |v_2\rangle &= |v_7\rangle = |v_8\rangle = |v_9\rangle = |1\rangle, \\ |v_3\rangle &= |2\rangle, \quad |v_4\rangle = |2\rangle + |3\rangle, \\ |v_5\rangle &= |2\rangle + 2|3\rangle, \quad |v_6\rangle = |2\rangle + 3|3\rangle. \end{aligned} \quad (11)$$

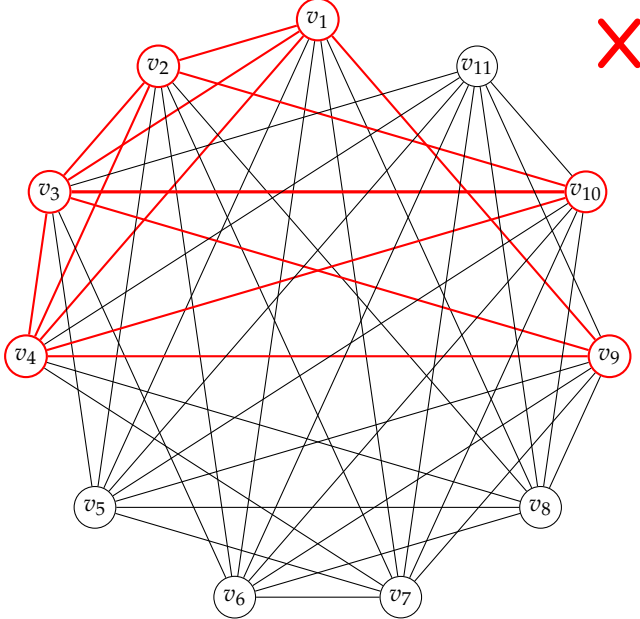


FIG. 12. The unique 11-vertex octic graph without C_5 as a subgraph. The graph does not admit a FOR(4) as $C_4^{(3)}$ is its induced subgraph (highlighted in red).

We have not been able to find the number of the connected graphs and we refer the reader to the database [59] for the cases $N \leq 22$, only noting here that for $N = 22$ this number is around 2.1×10^{29} .

V. CONCLUSIONS

We demonstrated that three-qutrit genuinely unextendible product bases (GUPBs) with the minimal theoretically permissible cardinality of thirteen do not exist. To this end, we exploited the recent characterization of local orthogonality graphs for GUPBs and employed a forbidden induced subgraph characterization to efficiently prune the set of

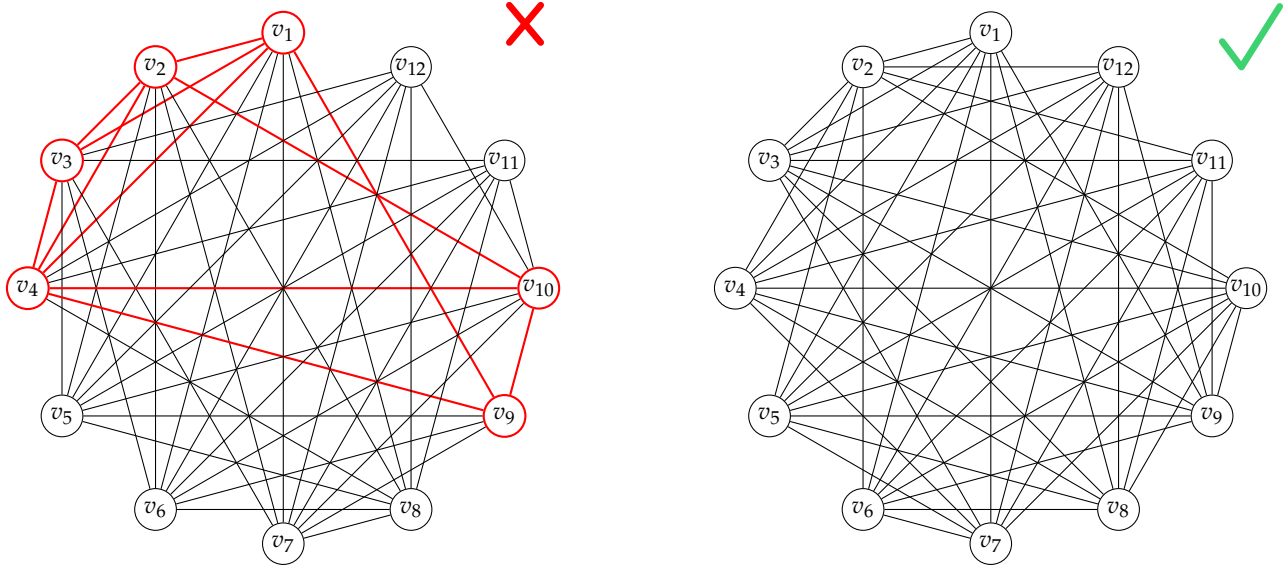


FIG. 13. (left) Forbidden induced subgraph E_6^1 (cf. Fig. 10) highlighted in graph L_{70} . (right) Graph L_{94} has FORs(4) with eight vectors spanning only a two dimensional subspace (see Sec. IV B 2).

candidate graphs. This approach allowed us to show that only two eligible graphs have orthogonal representations, yet neither of them exhibits the required spanning properties. We also discussed partial results concerning graphs associated with larger bases and systems involving ququart subsystems.

The proposed approach proved effective for small systems, but its direct application becomes increasingly challenging as system dimensions and sizes of the bases grow. The method thus calls for improvements allowing for treating graphs with more vertices. First, one should apply other methods (see, e.g., [60–62]) for the induced subgraph isomorphism problems. Second, one could also look into the possibility of graph elimination already at the construction stage of the candidate graphs, that is, instead of analyzing full graphs, smaller ones could be investigated and large sets of graphs could potentially be rejected early in the process. Nevertheless, it is rather clear that even a blend of such adjustments would still be profitable only in the problems of the limited scale. One must also bear in mind that the elimination of graphs is only part of the procedure — it is still necessary to verify whether every graph in the set obtained at some stage of the process admits FORs. If they do (i.e., we have constructed an obstruction set) these FORs must be characterized and their validity for GUPBs confirmed by checking certain properties, such as those outlined in Fact 1. It is likely that integrating advanced analytical tools with stronger graph characterizations—yet to be discovered—will be required. We believe that continued development along these lines may be key to overcoming the current limitations and advancing further the field.

VI. ACKNOWLEDGMENTS

The research was supported by Centre of Informatics Tricity Academic Supercomputer & Network (CI TASK) through the computing grant "Unextendible product bases and entangled subspaces".

[1] C. H. Bennett, D. P. DiVincenzo, T. Mor, P. W. Shor, J. A. Smolin, and B. M. Terhal, *Unextendible Product Bases and Bound Entanglement*, *Phys. Rev. Lett.* **82**, 5385 (1999).

[2] D. P. DiVincenzo, T. Mor, P. W. Shor, J. A. Smolin, B. M. Terhal, *Unextendible Product Bases, Uncompletable Product Bases and Bound Entanglement*, *Comm. Math. Phys.* **238**, 379 (2003).

[3] M. Horodecki, P. Horodecki, and R. Horodecki, *Mixed-State Entanglement and Distillation: Is there a "Bound" Entanglement in Nature?*, *Phys. Rev. Lett.* **80**, 5239 (1998).

[4] C. H. Bennett, D. P. DiVincenzo, C. A. Fuchs, T. Mor, E. Rains, P. W. Shor, J. A. Smolin, and W. K. Wootters, *Quantum nonlocality without entanglement*, *Phys. Rev. A* **59**, 1070 (1999).

[5] S. De Rinaldis, *Distinguishability of complete and unextendible product bases*, *Phys. Rev. A* **70**, 022309 (2004).

[6] J. Niset and N. J. Cerf, *Multipartite nonlocality without entanglement in many dimensions*, *Phys. Rev. A* **74**, 052103 (2006).

- [7] F. Shi, M.-Sh. Li, L. Chen, and Xi. Zhang *Strong quantum nonlocality for unextendible product bases in heterogeneous systems*, *J. Phys. A: Math. Theor.* **55**, 015305 (2022).
- [8] Yi. He, F. Shi, and Xi. Zhang, *Strong quantum nonlocality and unextendibility without entanglement in N-partite systems with odd N*, *Quantum* **8**, 1349 (2024).
- [9] R. Augusiak, J. Stasińska, C. Hadley, J. K. Korbicz, M. Lewenstein, A. Acín, *Bell inequalities with no quantum violation and unextendible product bases*, *Phys. Rev. Lett.* **107**, 070401 (2011).
- [10] R. Augusiak, T. Fritz, Ma. Kotowski, Mi. Kotowski, M. Pawłowski, M. Lewenstein, and A. Acín, *Tight Bell inequalities with no quantum violation from qubit unextendible product bases*, *Phys. Rev. A* **85**, 042113 (2012).
- [11] L. Chen and D. Z. Djokovic, *Nonexistence of n -qubit unextendible product bases of size $2^n - 5$* , *Quantum Inf Process* **17**, 24 (2018).
- [12] N. Johnston, *The Structure of Qubit Unextendible Product Bases*, *J. Phys. A: Math. Theor.* **47**:424034, 2014.
- [13] J. Chen and N. Johnston, *The minimum size of unextendible product bases in the bipartite case (and some multipartite cases)*, *Comm. Math. Phys.* **333**, 351 (2015).
- [14] L. Chen and D. Z. Djokovic, *Multiqubit UPB: The method of formally orthogonal matrices*, *J. Phys. A: Math. Theor.* **51** 265302 (2018).
- [15] K. Wang and L. Chen, *The construction of 7-qubit unextendible product bases of size ten*, *Quantum Inf Process* **19**, 185 (2020).
- [16] S. You, Ch. Wang, F. Shi, S. Hu. and Yi. Zhang, *Unextendible product bases from tile structures in bipartite systems*, *J. Phys. A: Math. Theor.* **56**, 015303 (2023).
- [17] Xi.-F. Zhen, H.-J. Zuo, F. Shi, and Sh.-M. Fei, *Unextendible and strongly uncompletable product bases*, *J. Math. Phys.* **65**, 112201 (2024).
- [18] F. Shi, M.-Sh. Li, and Qi Zhao, *Unextendible and uncompletable product bases in every bipartition*, *New J. Phys.* **24**, 113025 (2022).
- [19] M. Demianowicz, K. Vogtt, and R. Augusiak, *Completely entangled subspaces of entanglement depth k* , *Phys. Rev. A* **110**, 012403 (2024).
- [20] M. Demianowicz and R. Augusiak, *From unextendible product bases to genuinely entangled subspaces*, *Phys. Rev. A* **98**, 012312 (2018).
- [21] K. Wang, L. Chen, L. Zhao, and Y. Guo, *4×4 unextendible product basis and genuinely entangled space*, *Quantum Inf Process* **18**, 202 (2019).
- [22] M. Demianowicz, *Negative result about the construction of genuinely entangled subspaces from unextendible product bases*, *Phys. Rev. A* **106**, 012442 (2022).
- [23] F. Shi, G. Bai, X. Zhang, Q. Zhao, and G. Chiribella, *Graph-theoretic characterization of unextendible product bases*, *Phys. Rev. Research* **5**, 033144 (2023).
- [24] N. Alon and L. Lovász, *Unextendible Product Bases*, *J. Combinatorial Theory, Ser. A* **95**, 169 (2001).
- [25] K. Feng, *Unextendible product bases and 1-factorization of complete graphs*, *Discr. App. Math.* **154**, 942 (2006).
- [26] K. Parthasarathy, *On the maximal dimension of a completely entangled subspace for finite level quantum systems*, *Proceedings Mathematical Sciences* **114**, 365 (2004).
- [27] B. V. R. Bhat, *A completely entangled subspace of maximal dimension*, *Int. J. Quantum Inf.* **4**, 325 (2006).
- [28] J. Walgate and A. J. Scott, *Generic local distinguishability and completely entangled subspaces*, *J. Phys. A* **41**, 375305 (2008).
- [29] T. Cubitt, A. Montanaro, and A. Winter, *On the dimension of subspaces with bounded Schmidt rank*, *J. Math. Phys.* **49**, 022107 (2008).
- [30] N. Johnston, B. Lovitz, and A. Vijayaraghavan, *A Complete Hierarchy of Linear Systems for Certifying Quantum Entanglement of Subspaces*, *Phys. Rev. A* **106**, 062443 (2022).
- [31] H. Derkzen, N. Johnston, and B. Lovitz, *X-arability of mixed quantum states*, *arXiv:2409.18948v2* (2024).
- [32] S. Agrawal, S. Halder, and M. Banik, *Genuinely entangled subspace with all-encompassing distillable entanglement across every bipartition*, *Phys. Rev. A* **99**, 032335 (2019).
- [33] M. Demianowicz and R. Augusiak, *Entanglement of genuinely entangled subspaces and states: Exact, approximate, and numerical results*, *Phys. Rev. A* **100**, 062318 (2019).
- [34] M. Demianowicz and R. Augusiak, *An approach to constructing genuinely entangled subspaces of maximal dimension*, *Quant. Inf. Proc.* **19**, 199 (2020).
- [35] O. Makuta, B. Kuzaka, and R. Augusiak, *Fully non-positive-partial-transpose genuinely entangled subspaces*, *Quantum* **7**, 915 (2023).
- [36] M. Demianowicz, *Universal construction of genuinely entangled subspaces of any size*, *Quantum* **6**, 854 (2022).
- [37] F. Shi, M.-S. Li, X. Zhang, and Q. Zhao, *Unextendible and uncompletable product bases in every bipartition*, *New J. Phys.* **24**, 113025 (2022).
- [38] J. A. Bondy and U. S. R. Murty, *Graph theory* (Springer, London, 2008).
- [39] AIM Minimum Rank – Special Graphs Work Group (F. Barioli, W. Barrett, S. Butler, S. M. Cioabă, D. Cvetković, S. M. Fallat, C. Godsil, W. Haemers, L. Hogben, R. Mikkelson, S. Narayan, O. Pryporova, I. Sciriha, W. So, D. Stevanović, H. van der Holst, K. Vander Meulen, and A. Wangsness), *Zero forcing sets and the minimum rank of graphs*, *Linear Algebra and its Applications* **428**, 1628 (2008).
- [40] M. Booth, P. Hackney, B. Harris, Ch. R. Johnson, M. Lay, L. H. Mitchell, S. K. Narayan, A. Pascoe, K. Steinmetz, B. D. Sutton, and W. Wang, *On the Minimum Rank Among Positive Semidefinite Matrices with a Given Graph*, *SIAM Journal on Matrix Analysis and Applications* **30**, 731 (2008).
- [41] L. Lovász, *On the Shannon capacity of a graph*, *IEEE Transactions on Information Theory* **25**, 1 (1979).
- [42] A. Brandstädt, V. B. Le, and J. P. Spinrad, *Graph Classes: A Survey* (chapter 7), SIAM Monographs on Discrete Mathematics and Applications (Society for Industrial and Applied Mathematics, 1999), .

[43] M. Chudnovsky, N. Robertson, P. Seymour, and R. Thomas, *The strong perfect graph theorem*, *Annals of Mathematics*, **164**, 51 (2006).

[44] G. Durán, *Forbidden induced subgraph characterizations of subclasses and variations of perfect graphs: A survey*, *Electronic Notes in Discrete Mathematics* **44**, 399 (2013).

[45] oeis.org/A033301.

[46] oeis.org/A033483.

[47] oeis.org/A006820.

[48] M. Meringer, *Fast generation of regular graphs and construction of cages*, *J. Graph Theory* **30**, 137 (1999).

[49] mathe2.uni-bayreuth.de/markus/reggraphs.html.

[50] M. Demianowicz, *Supplementary material to "Progress in the study of the (non)existence of genuinely unextendible product bases"*, Zenodo (2025).

[51] oeis.org/A002851.

[52] oeis.org/A165653.

[53] oeis.org/A006821.

[54] oeis.org/A165655.

[55] oeis.org/A014377.

[56] oeis.org/A165877.

[57] oeis.org/A165878.

[58] P. Turán, *On an extremal problem in graph theory (in Hungarian)*, *Math. Fiz. Lapok* **48**, 436 (1941).

[59] oeis.org/A014378.

[60] S. Wernicke, *Efficient Detection of Network Motifs*, *IEEE/ACM Transactions on Computational Biology and Bioinformatics* **3**, 347 (2006).

[61] J. A. Grochow and M. Kellis, *Network Motif Discovery Using Subgraph Enumeration and Symmetry-Breaking*, in: T. Speed, H. Huang (eds), *Research in Computational Molecular Biology. RECOMB 2007. Lecture Notes in Computer Science()*, **4453**, (Springer, Berlin, Heidelberg, 2007).

[62] P. M. P. Ribeiro and F. M. A. Silva, *g-tries: an efficient data structure for discovering network motifs*, in: S. Y. Shin, S. Ossowski, M. Schumacher, M. J. Palakal, and Ch.-Ch. Hung (eds), *SAC '10: Proceedings of the 2010 ACM Symposium on Applied Computing* (Sierre, Switzerland, 2010).

[63] F. Barioli, W. Barrett, S. M. Fallat, H. T. Hall, L. Hogben, B. Shader, P. van den Driessche, and H. van der Holst, *Parameters Related to Tree-Width, Zero Forcing, and Maximum Nullity of a Graph*, *J. Graph Theory* **72**, 146 (2013).

Appendix A: 3-ladder graph

Here we consider the 3-ladder graph L_6 , see Fig. 14.

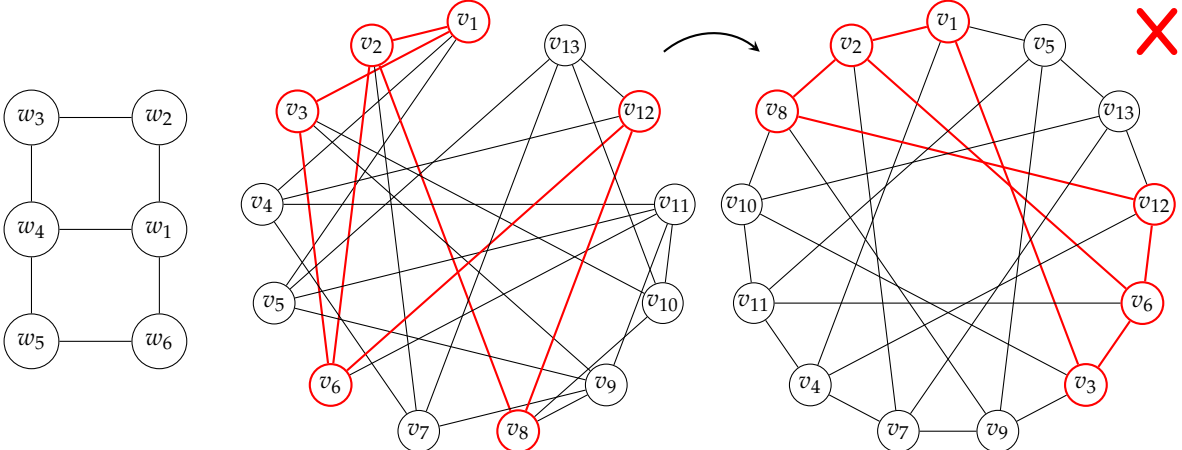


FIG. 14. (left) 3-ladder graph L_6 — a 6-vertex graph without a $\text{FOR}(3)$ [Lemma 6]. (middle) L_6 highlighted in M_{10778} . (right) M_{10778} is isomorphic to a circulant graph; the graph shows the vertices rearranged to better visualize it.

Lemma 6. L_6 does not admit a $\text{FOR}(3)$.

Proof. It follows from Lemma 1 that it necessarily holds that $|w_2\rangle = |w_4\rangle$ or $|w_3\rangle = |w_5\rangle$. None of these cases is possible, though, as $\mathcal{N}(w_2) \neq \mathcal{N}(w_4)$ and $\mathcal{N}(w_3) \neq \mathcal{N}(w_5)$. \square

The adjacency matrix for the graph is

$$\mathcal{A}(L_6) = \begin{pmatrix} 0 & 1 & 0 & 1 & 0 & 1 \\ 1 & 0 & 1 & 0 & 0 & 0 \\ 0 & 1 & 0 & 1 & 0 & 0 \\ 1 & 0 & 1 & 0 & 1 & 0 \\ 0 & 0 & 0 & 1 & 0 & 1 \\ 1 & 0 & 0 & 0 & 1 & 0 \end{pmatrix}. \quad (\text{A1})$$

Appendix B: Analysis of graphs from Eq. (8)

Here we analyze the 14-vertex 4-regular graphs not discarded by \mathcal{O}_3 [cf. Eq. 8]; they are depicted in Fig. 15. We will now show that there is only a single graph among them not having a FOR(3).

1. Graph N_{2359}

An exemplary FOR(3) is as follows:

$$\begin{aligned} |v_1\rangle &= |0\rangle, & |v_2\rangle &= |1\rangle, \\ |v_3\rangle &= |v_4\rangle = |v_5\rangle = |2\rangle, \\ |v_6\rangle &= |0\rangle + 2|1\rangle, & |v_7\rangle &= |0\rangle - |1\rangle, \\ |v_8\rangle &= 2|0\rangle - |1\rangle + 4|2\rangle, & |v_9\rangle &= |0\rangle + |1\rangle - |2\rangle, \\ |v_{10}\rangle &= |v_{11}\rangle = |v_{12}\rangle = |0\rangle - 2|1\rangle - |2\rangle, \\ |v_{13}\rangle &= 7|0\rangle + 4|1\rangle - |2\rangle, & |v_{14}\rangle &= |0\rangle + |1\rangle - 3|2\rangle. \end{aligned} \quad (\text{B1})$$

It is evident that it necessarily holds $|v_3\rangle = |v_4\rangle = |v_5\rangle$ (vertices marked in brown in Fig. 15) and $|v_{10}\rangle = |v_{11}\rangle = |v_{12}\rangle$ (lime vertices) in any FOR(3) of N_{2359} . In turn, this graph cannot be a LOG for a GUPB as it violates Fact 1, because $\dim \text{span}\{|v_3\rangle, |v_4\rangle, |v_5\rangle, |v_{10}\rangle, |v_{11}\rangle, |v_{12}\rangle\} = 2$.

2. Graph N_{11743}

A FOR(3) for the graph is:

$$\begin{aligned} |v_1\rangle &= |0\rangle, \\ |v_2\rangle &= |v_5\rangle = |1\rangle, \\ |v_3\rangle &= |v_4\rangle = |2\rangle, \\ |v_6\rangle &= |0\rangle + |2\rangle, & |v_7\rangle &= |0\rangle + |1\rangle, \\ |v_8\rangle &= |v_9\rangle = |0\rangle + 2|1\rangle - |2\rangle, \\ |v_{10}\rangle &= |v_{11}\rangle = |0\rangle - |1\rangle + |2\rangle, \\ |v_{12}\rangle &= |v_{13}\rangle = |v_{14}\rangle = |0\rangle - 2|1\rangle - 3|2\rangle. \end{aligned} \quad (\text{B2})$$

Considering relevant diamond graphs, we immediately find that $|v_2\rangle = |v_5\rangle$ (lime vertices) and $|v_3\rangle = |v_4\rangle$ (brown vertices) in any FOR(3). Further, considering the square graphs with vertices $(v_8, v_{10}, v_{13}, v_{14})$ and $(v_9, v_{11}, v_{12}, v_{14})$ and the relevant neighborhoods we find $|v_{12}\rangle = |v_{13}\rangle = |v_{14}\rangle$ (blue vertices). Similar consideration for the square graphs (v_6, v_8, v_9, v_{14}) and $(v_7, v_{10}, v_{11}, v_{14})$ gives, respectively, $|v_8\rangle = |v_9\rangle$ (gray) and $|v_{10}\rangle = |v_{11}\rangle$ (violet). These FORs are admissible by Fact 1.

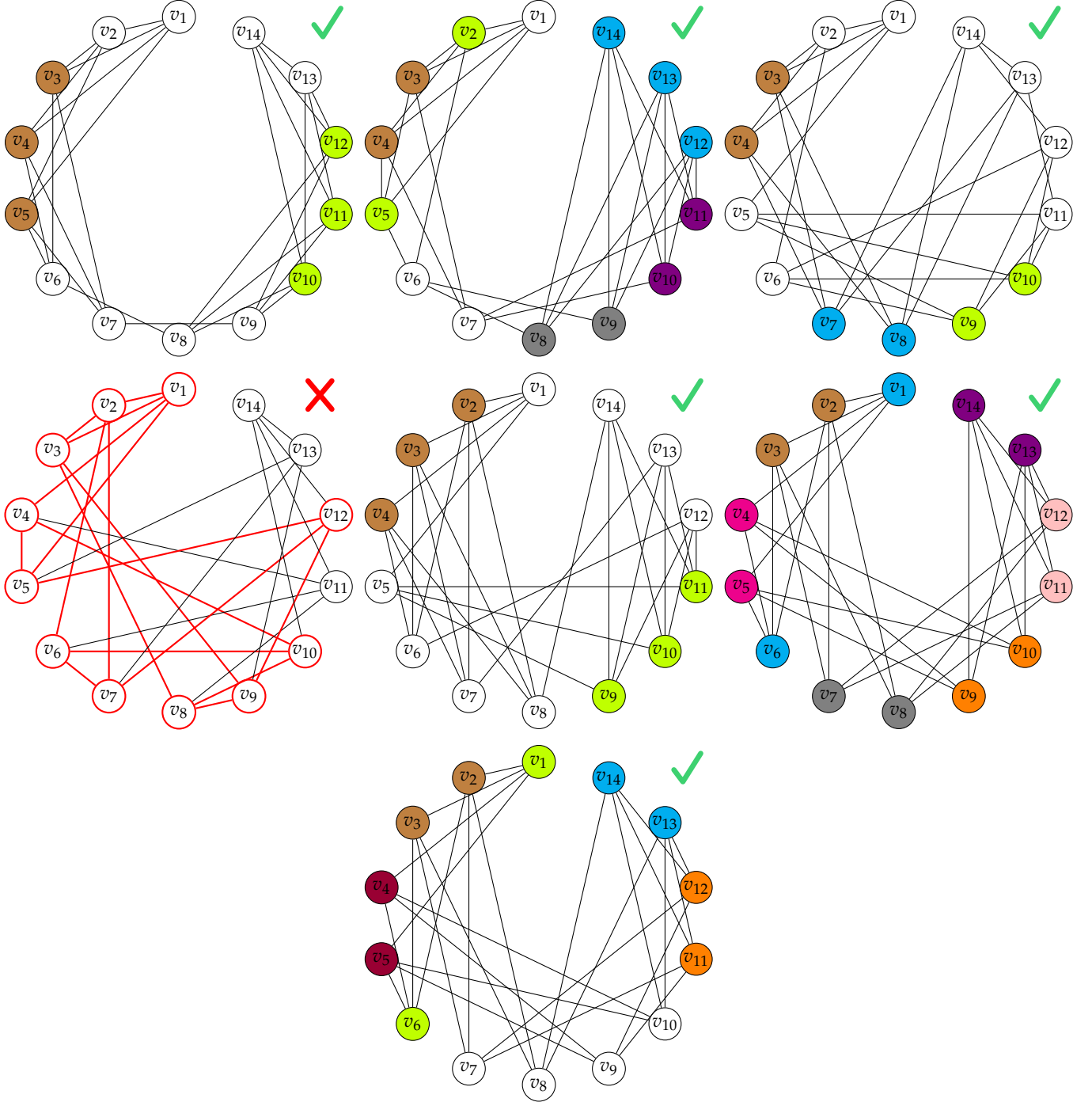


FIG. 15. The seven graphs not eliminated by \mathcal{O}_3 in case of 14-vertex 4-regular graphs. First row (from the left): N_{2359} , N_{11743} , N_{36919} ; second row (from the left): N_{80015} , N_{87949} , N_{87956} ; third row: N_{87957} . Only one of these graphs – N_{80015} – does not admit a $\text{FOR}(3)$; a forbidden induced subgraph is highlighted in red (\hat{N}_{11} , see Appendix B.4). Same color vertices in a graph have necessarily identical vectors in a $\text{FOR}(3)$ (see the main text).

3. Graph N_{36919}

A FOR(3) is given by the following set of vectors:

$$\begin{aligned}
 |v_1\rangle &= |0\rangle, & |v_2\rangle &= |1\rangle, \\
 |v_3\rangle &= |v_4\rangle = |2\rangle, \\
 |v_5\rangle &= |1\rangle - x|2\rangle, & |v_6\rangle &= |0\rangle - |2\rangle, \\
 |v_7\rangle &= |v_8\rangle = |0\rangle - |1\rangle, \\
 |v_9\rangle &= |v_{10}\rangle = |0\rangle + x|1\rangle + |2\rangle, \\
 |v_{11}\rangle &= (1 + x^2)|0\rangle - x|1\rangle - |2\rangle, \\
 |v_{12}\rangle &= x|0\rangle - 2|1\rangle + x|2\rangle, \\
 |v_{13}\rangle &= (x - 2)|0\rangle + (x - 2)|1\rangle + 2x|2\rangle, \\
 |v_{14}\rangle &= x|0\rangle + x|1\rangle - (x - 2)|2\rangle,
 \end{aligned} \tag{B3}$$

where x is the real solution of $x^3 - 3x^2 + x - 2 = 0$, which is found with standard methods to be

$$x = 1 + \sqrt[3]{\frac{3}{2} + \sqrt{\frac{211}{108}}} + \sqrt[3]{\frac{3}{2} - \sqrt{\frac{211}{108}}} \simeq 2.89329 \tag{B4}$$

It is trivial to see that $|v_3\rangle = |v_4\rangle$ (brown vertices), $|v_7\rangle = |v_8\rangle$ (blue), and $|v_9\rangle = |v_{10}\rangle$ (lime) in any FOR(3).

We have not found any argument either supporting or refuting this graph's validity as a candidate LOG. Nevertheless, among the graphs considered, it appears to be the most promising, as it has the fewest repeated vectors—only three in total.

4. Graph N_{80015}

This graph has an appealing structure, which may not be that easy to infer from its form shown in Fig. 15. To show non-existence of a FOR(3) for this graph, we consider its 11-vertex induced subgraph with vertices $(v_1, v_2, v_3, v_4, v_5, v_6, v_7, v_8, v_9, v_{10}, v_{12})$ (see Fig. 16); we will call it \hat{N}_{11} .

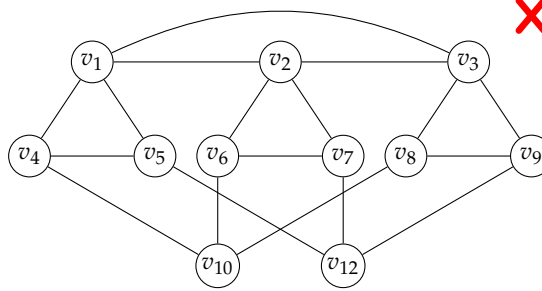


FIG. 16. Induced subgraph \hat{N}_{11} of graph N_{80015} without a FOR(3).

Let $|v_1\rangle = |0\rangle$, $|v_2\rangle = |1\rangle$, and $|v_3\rangle = |2\rangle$. We then have

$$\begin{aligned}
 |v_4\rangle &= |1\rangle + x|2\rangle, & |v_5\rangle &= x^*|1\rangle - |2\rangle, \\
 |v_6\rangle &= |0\rangle + y|2\rangle, & |v_7\rangle &= y^*|0\rangle - |2\rangle, \\
 |v_8\rangle &= |0\rangle + z|1\rangle, & |v_9\rangle &= z^*|0\rangle - |1\rangle.
 \end{aligned} \tag{B5}$$

with $x, y, z \neq 0$. Further, it must hold

$$\dim \text{span}\{|v_4\rangle, |v_6\rangle, |v_8\rangle\} = \dim \text{span}\{|v_5\rangle, |v_7\rangle, |v_9\rangle\} = 2. \tag{B6}$$

We thus obtain conditions:

$$\begin{vmatrix} 0 & 1 & 1 \\ 1 & 0 & z \\ x & y & 0 \end{vmatrix} = xz + y = 0, \quad \begin{vmatrix} 0 & y^* & z^* \\ x^* & 0 & -1 \\ -1 & -1 & 0 \end{vmatrix} = -x^*z^* + y^* = 0, \tag{B7}$$

which are contradictory under our assumptions. Graph \hat{N}_{11} constitutes a forbidden induced subgraph.

5. Graph N_{87949}

A FOR(3) for the graph in question is:

$$\begin{aligned} |v_1\rangle &= |0\rangle, & |v_2\rangle &= |v_3\rangle = |v_4\rangle = |1\rangle, \\ |v_5\rangle &= |1\rangle - |2\rangle, & |v_6\rangle &= 5|0\rangle - |2\rangle, & |v_7\rangle &= 3|0\rangle - |2\rangle, & |v_8\rangle &= 2|0\rangle - |2\rangle, \\ |v_9\rangle &= |v_{10}\rangle = |v_{11}\rangle = |0\rangle - |1\rangle - |2\rangle, \\ |v_{12}\rangle &= |0\rangle - 4|1\rangle + 5|2\rangle, & |v_{13}\rangle &= |0\rangle - 2|1\rangle + 3|2\rangle, & |v_{14}\rangle &= |0\rangle - |1\rangle + 2|2\rangle. \end{aligned} \quad (\text{B8})$$

Considering the square graph with vertices (v_3, v_4, v_6, v_7) we find that $|v_3\rangle = |v_4\rangle$ or/and $|v_6\rangle = |v_7\rangle$. Since $\mathcal{N}(v_6) \neq \mathcal{N}(v_7)$, we conclude $|v_3\rangle = |v_4\rangle$. Similar reasoning for the square graph (v_2, v_3, v_6, v_7) leads to $|v_2\rangle = |v_3\rangle$, and in turn $|v_2\rangle = |v_3\rangle = |v_4\rangle$ (brown vertices). Analogous consideration for the square graphs $(v_9, v_{10}, v_{13}, v_{14})$ and $(v_9, v_{10}, v_{12}, v_{13})$ results in $|v_9\rangle = |v_{10}\rangle = |v_{11}\rangle$ (lime vertices). This necessarily holds in any FOR(3) of the graph, eliminating it – by Fact 1 – from the set of candidate LOGs for GUPBs, as $\dim \text{span}\{|v_2\rangle, |v_3\rangle, |v_4\rangle, |v_9\rangle, |v_{10}\rangle, |v_{11}\rangle\} = 2$.

6. Graph N_{87956}

This graph has very simple FORs(3). An exemplary one is as follows:

$$\begin{aligned} |v_1\rangle &= |v_6\rangle = |0\rangle, & |v_2\rangle &= |v_3\rangle = |1\rangle, \\ |v_4\rangle &= |v_5\rangle = 2|1\rangle - |2\rangle, & |v_7\rangle &= |v_8\rangle = |0\rangle + |2\rangle, \\ |v_9\rangle &= |v_{10}\rangle = |0\rangle - |1\rangle - 2|2\rangle, \\ |v_{11}\rangle &= |v_{12}\rangle = 4|0\rangle - |1\rangle - 4|2\rangle, \\ |v_{13}\rangle &= |v_{14}\rangle = 2|0\rangle - 4|1\rangle + 3|2\rangle, \end{aligned} \quad (\text{B9})$$

Consideration of the following square graphs and relevant neighborhoods gives the properties holding for any FOR(3) (we first give the vertices of the square graph and then the consequence): $(v_2, v_3, v_6, v_7) — |v_2\rangle = |v_3\rangle$ (brown vertices), $(v_1, v_3, v_4, v_6) — |v_1\rangle = |v_6\rangle$ (blue); $(v_9, v_{11}, v_{13}, v_{14}) — |v_{13}\rangle = |v_{14}\rangle$ (violet), $(v_3, v_7, v_8, v_{12}) — |v_7\rangle = |v_8\rangle$ (gray), $(v_4, v_9, v_{10}, v_{13}) — |v_9\rangle = |v_{10}\rangle$ (orange), $(v_1, v_4, v_5, v_9) — |v_4\rangle = |v_5\rangle$ (magenta), $(v_7, v_{11}, v_{12}, v_{14}) — |v_{11}\rangle = |v_{12}\rangle$ (pink). The FORs are not filtered out by Fact 1.

7. Graph N_{87957}

A FOR(3) for this graph is:

$$\begin{aligned} |v_1\rangle &= |v_6\rangle = |0\rangle, & |v_2\rangle &= |v_3\rangle = |1\rangle, & |v_4\rangle &= |v_5\rangle = 2|1\rangle - |2\rangle, \\ |v_7\rangle &= |0\rangle + |2\rangle, & |v_8\rangle &= 7|0\rangle - 12|2\rangle, \\ |v_9\rangle &= |0\rangle - 2|1\rangle - 4|2\rangle, & |v_{10}\rangle &= |0\rangle - |1\rangle - 2|2\rangle, \\ |v_{11}\rangle &= |v_{12}\rangle = 2|0\rangle + 5|1\rangle - 2|2\rangle, \\ |v_{13}\rangle &= |v_{14}\rangle = 12|0\rangle - 2|1\rangle + 7|2\rangle. \end{aligned} \quad (\text{B10})$$

As above, we consider the square graphs and find the following properties (using the above notation): $(v_1, v_2, v_4, v_6) — |v_1\rangle = |v_6\rangle$ (lime), $(v_2, v_3, v_7, v_8) — |v_2\rangle = |v_3\rangle$ (brown), $(v_4, v_5, v_9, v_{10}) — |v_4\rangle = |v_5\rangle$ (violet), $(v_7, v_9, v_{11}, v_{12}) — |v_{11}\rangle = |v_{12}\rangle$ (orange), $(v_{10}, v_{11}, v_{13}, v_{14}) — |v_{13}\rangle = |v_{14}\rangle$, which are necessarily shared by any FOR(3). The FORs are permissible by Fact 1.

Appendix C: 14-vertex 3-regular graphs

Here, we provide a brief analysis of the candidate fourteen-vertex three-regular graphs (see Sec. IV A 2).

1. Connected graphs

We first analyze the connected graphs defined by set $\mathcal{O}_3 \setminus C_4$.

a. Girth-3 graphs

These are graphs with the following GENREG indices: 5, 14, 17, 254, 264, 265, 267, 269, 270, 271, 272, 275, 276, 288, 289, 292, 293, 294, 301, 305, 306, 308, 310, 313, 314, 320, 322, 341, 342, 353, 354, 364, 367, 370, 372, 374, 382, 388, 389, 393, 397, 399. They all have permissible FORs(3).

In Fig. 17, we show graph 254 for which a FOR(3) is as follows:

$$\begin{aligned}
 |v_1\rangle &= |0\rangle, & |v_2\rangle &= |1\rangle, & |v_3\rangle &= |2\rangle, & |v_4\rangle &= 2|1\rangle - 3|2\rangle, \\
 |v_5\rangle &= |0\rangle + |2\rangle, & |v_6\rangle &= 2|0\rangle - |1\rangle, & |v_7\rangle &= |v_8\rangle = 2|0\rangle - 3|1\rangle - |2\rangle, \\
 |v_9\rangle &= |v_{10}\rangle = |0\rangle + 2|1\rangle - 3|2\rangle, & |v_{11}\rangle &= 4|0\rangle + 2|1\rangle + |2\rangle, \\
 |v_{12}\rangle &= |v_{13}\rangle = |0\rangle + |1\rangle + |2\rangle, & |v_{14}\rangle &= |0\rangle - 3|1\rangle + 2|2\rangle.
 \end{aligned} \tag{C1}$$

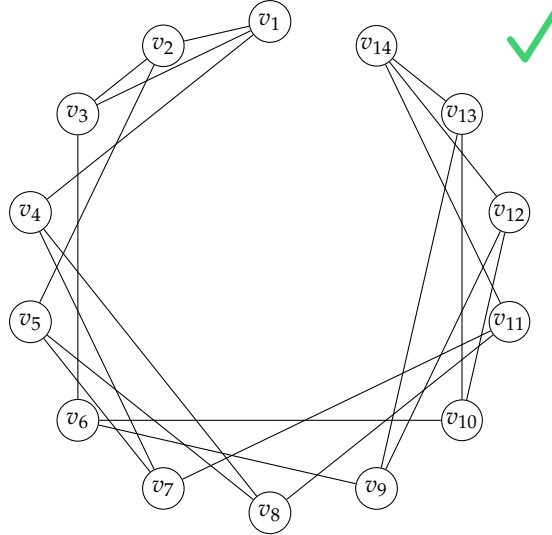


FIG. 17. Graph 254 – one of the 14-vertex 3-regular graphs with $g = 3$. The graph has a FOR(3) shown in Eq. (C1).

b. Girth-4 graphs

These are graphs with the following GENREG indices 400, 401, 402, 406, 411, 421. We have found that all of them have permissible FORs(3).

In Fig. 18, we show graph 411 for which a FOR(3) is as follows:

$$\begin{aligned}
 |v_1\rangle &= |0\rangle, & |v_2\rangle &= |v_3\rangle = |1\rangle, & |v_4\rangle &= |1\rangle - |2\rangle, & |v_5\rangle &= 2|0\rangle - |2\rangle, \\
 |v_6\rangle &= 4|0\rangle - |2\rangle, & |v_7\rangle &= 5|0\rangle - |1\rangle - |2\rangle, & |v_8\rangle &= |0\rangle - |1\rangle - |2\rangle, \\
 |v_9\rangle &= |0\rangle + 3|1\rangle + 2|2\rangle, & |v_{10}\rangle &= |0\rangle + |1\rangle + 4|2\rangle, & |v_{11}\rangle &= |v_{12}\rangle = |0\rangle + |1\rangle, \\
 |v_{13}\rangle &= |0\rangle - |1\rangle + |2\rangle, & |v_{14}\rangle &= |0\rangle - |1\rangle.
 \end{aligned} \tag{C2}$$

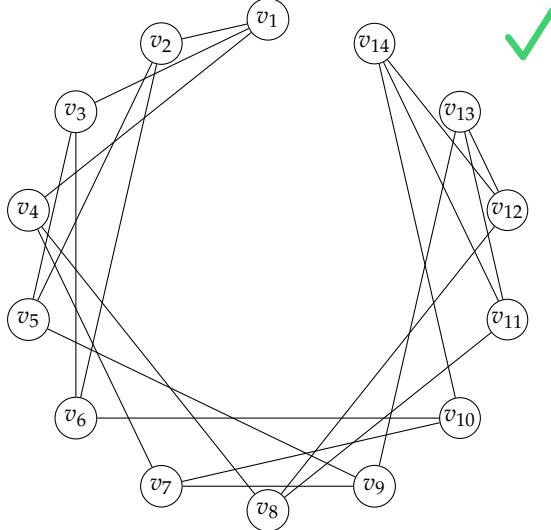


FIG. 18. Graph 411 – one of the 14-vertex 3-regular graphs with $g = 4$. The graph has a FOR(3) shown in Eq. (C2).

c. *Girth-5 graphs*

We found that all the eight graphs (indices 501 – 508 in GENREG) have permissible FORs(3). We give an exemplary representation for graph 501 (see Fig. 19):

$$\begin{aligned}
 |v_1\rangle &= |0\rangle, & |v_2\rangle &= |1\rangle, & |v_3\rangle &= |1\rangle - 2|2\rangle, & |v_4\rangle &= |1\rangle - |2\rangle, \\
 |v_5\rangle &= 3|0\rangle - 2|2\rangle, & |v_6\rangle &= |0\rangle + 2|2\rangle, & |v_7\rangle &= 2|0\rangle + 6|1\rangle + 3|2\rangle, \\
 |v_8\rangle &= 2|0\rangle - 2|1\rangle - |2\rangle, & |v_9\rangle &= 2|0\rangle + 3|1\rangle + 3|2\rangle, & |v_{10}\rangle &= |0\rangle - 3|1\rangle - 3|2\rangle, \\
 |v_{11}\rangle &= 6|0\rangle + 5|1\rangle - 3|2\rangle, & |v_{12}\rangle &= 3|0\rangle - 3|1\rangle + 4|2\rangle, & |v_{13}\rangle &= |0\rangle + |1\rangle, & |v_{14}\rangle &= 3|0\rangle - 3|1\rangle + |2\rangle.
 \end{aligned} \tag{C3}$$

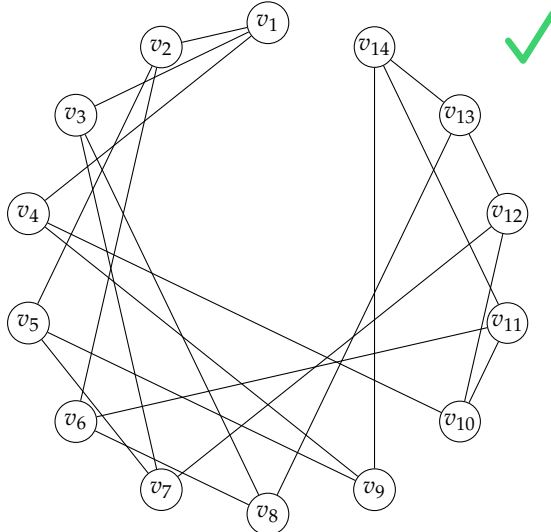


FIG. 19. One of the eight girth-5 3-regular graphs on 14 vertices; a FOR(3) for this graph is given in Eq. (C4).

d. *Girth-6 graph — Heawood graph*

The Heawood graph (graph number 509 in GENREG) is the unique $(3, 6)$ -cage, i.e., it is the smallest 3-regular graph with girth $g = 6$. We show this graph in Fig. 20. It follows from Ref. [63] that the minimal dimension for a FOR with real vectors is $d = 4$. An exemplary one is as follows:

$$\begin{aligned} |v_1\rangle &= |0\rangle, & |v_2\rangle &= 14|1\rangle + 7|2\rangle - 4|3\rangle, & |v_3\rangle &= 3|1\rangle - 2|2\rangle, & |v_4\rangle &= |1\rangle, \\ |v_5\rangle &= 2|0\rangle - 2|1\rangle - 7|3\rangle, & |v_6\rangle &= 10|0\rangle - 22|1\rangle + 32|2\rangle - 21|3\rangle, & |v_7\rangle &= 5|0\rangle + 2|1\rangle + 3|2\rangle, \\ |v_8\rangle &= |0\rangle + 2|1\rangle + 3|2\rangle, & |v_9\rangle &= |0\rangle - 2|2\rangle - |3\rangle, & |v_{10}\rangle &= |0\rangle + |2\rangle, \\ |v_{11}\rangle &= 2|0\rangle - 5|1\rangle + 2|3\rangle, & |v_{12}\rangle &= |0\rangle + |1\rangle - |2\rangle, & |v_{13}\rangle &= |0\rangle - |1\rangle - |2\rangle, & |v_{14}\rangle &= 2|0\rangle - |1\rangle + 2|3\rangle. \end{aligned} \quad (\text{C4})$$

We have not been able to verify whether the complex case also requires four dimensions. However, in view of the results of Ref. [63] it is likely that this is indeed the case.

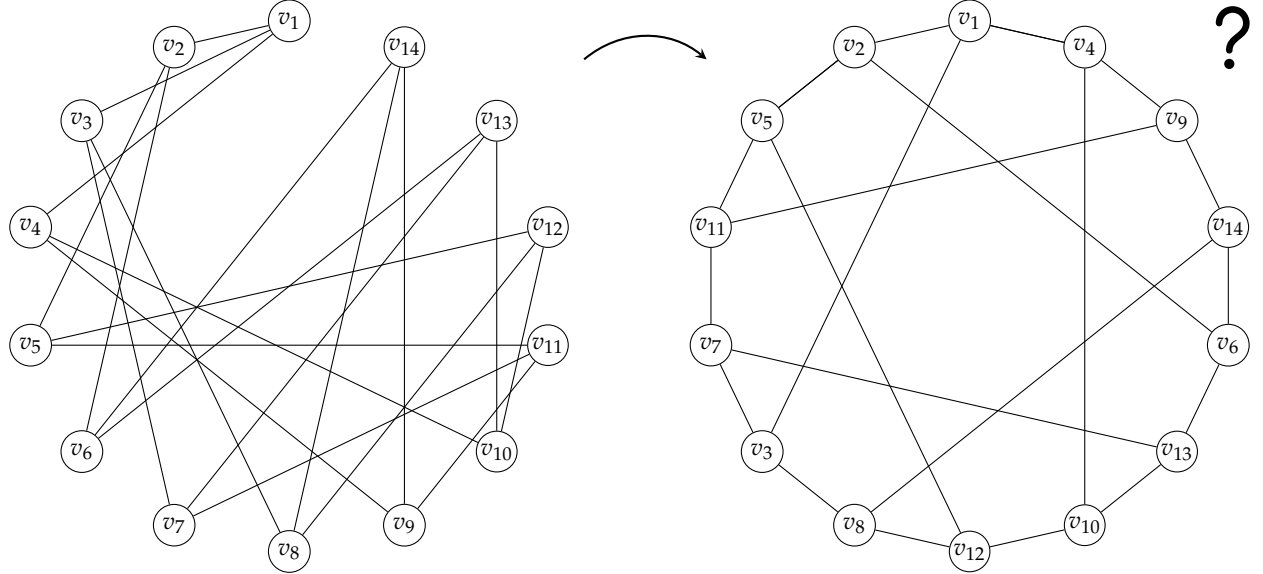


FIG. 20. The Heawood graph in the GENREG form (left) and in a more common layout (right). The minimal dimension for a real FOR is $d = 4$ [see Eq. (C4)]; it is not clear whether this is also the minimal dimension for the complex case.

2. Disconnected graphs

As noted in the main text, only type (b) graphs ($6 + 8$ vertices) need a more detailed investigation. We need to analyze (i) 6-vertex and (ii) 8-vertex 3-regular graphs. (i) There are two graphs in this category. We find that the house graph H_5 is an induced subgraph of the first one. The second one is the complete bipartite graph $K_{3,3}$ (also called the utility graph). It actually admits a FOR(2) and in any FOR(d) there is at least one three-tuple of identical vectors (cf. Sec. IV A 1, where $K_{4,4}$ is analyzed). (ii) This category consists of five graphs. We find that $\{K_5, L_6\}$ is an obstruction set defining a single graph having a FOR(3) — graph number 3, denote it P_3 (see Fig. 21). An exemplary FOR(3) of P_3 is as follows:

$$\begin{aligned} |v_1\rangle &= |0\rangle, & |v_2\rangle &= |1\rangle, & |v_3\rangle &= |2\rangle, \\ |v_4\rangle &= |1\rangle - |2\rangle, & |v_5\rangle &= |0\rangle + |2\rangle, & |v_6\rangle &= |0\rangle + |1\rangle, \\ |v_7\rangle &= |v_8\rangle = |0\rangle - |1\rangle - |2\rangle. \end{aligned} \quad (\text{C5})$$

It immediately follows that $|v_7\rangle = |v_8\rangle$ holds for any FOR(3) of P_3 leading to the elimination of $K_{3,3} + P_3$ as a LOG.

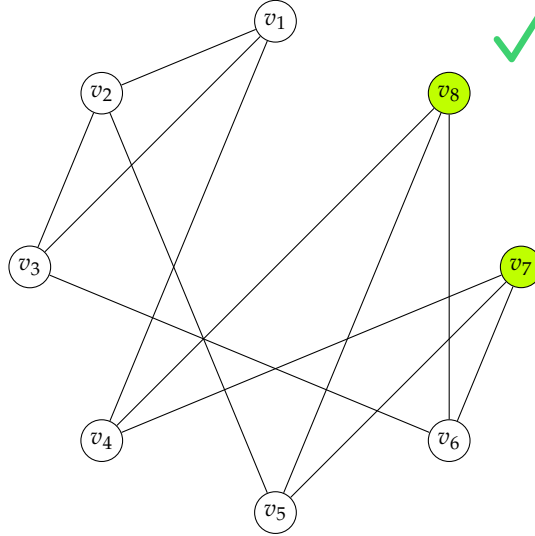


FIG. 21. The only 8-vertex 3-regular graph with a FOR(3), see Eq. (C5). Vectors corresponding to colored vertices are necessarily the same.

3. Petersen graph

As an addition to the analysis of the fourteen-vertex three-regular graphs, we also consider the Petersen graph. The Petersen graph (see Fig. 22) is the unique $(3, 5)$ -cage. It is a ten-vertex graph, which has a FOR(3) and we show one below:

$$\begin{aligned}
 |v_1\rangle &= |1\rangle, & |v_2\rangle &= |0\rangle, & |v_3\rangle &= 2|1\rangle + 3|2\rangle, & |v_4\rangle &= 2|0\rangle + 3|1\rangle - 2|2\rangle, \\
 |v_5\rangle &= |0\rangle + |2\rangle, & |v_6\rangle &= |0\rangle - |1\rangle - |2\rangle, & |v_7\rangle &= 2|0\rangle + |2\rangle, \\
 |v_8\rangle &= |1\rangle - |2\rangle, & |v_9\rangle &= |0\rangle + 3|1\rangle - 2|2\rangle, & |v_{10}\rangle &= |0\rangle - 2|1\rangle - 2|2\rangle,
 \end{aligned} \tag{C6}$$

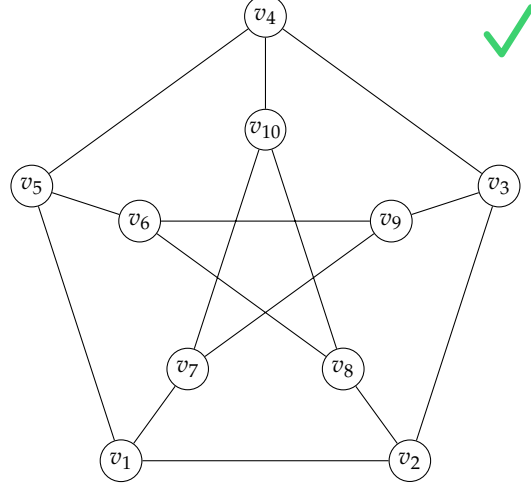


FIG. 22. Petersen graph; the graph admits a FOR(3), see Eq. (C6).

Appendix D: Thirteen-vertex four-regular graphs with the considered induced subgraphs

Table III below provides indices of graphs M_i admitting certain induced subgraphs. Ladder graph L_6 (see Appendix A), which does not belong to the obstruction set \mathcal{O}_3 [Eq. (5)], has been included.

forbidden induced subgraph	# graphs w/ induced subgraph	indices of graphs with induced subgraph
4-clique C_4	671	1 – 401, 439, 449, 511, 517, 537, 568, 578, 606, 618, 643, 686, 700, 716, 740, 774, 781, 867, 882, 931, 945, 956, 1164, 1166, 1316, 1343, 1350 – 1594
A-graph A_6	10 672	5 – 7, 9 – 10, 12 – 14, 16 – 24, 26 – 30, 32, 34, 38 – 47, 49, 51, 53 – 55, 57 – 67, 69 – 71, 75 – 83, 85 – 115, 117 – 121, 123 – 125, 128 – 196, 198 – 239, 243 – 278, 280 – 286, 288 – 329, 331 – 332, 335 – 336, 338 – 361, 363 – 396, 398 – 401, 406 – 422, 425, 427, 429 – 430, 432 – 434, 436 – 440, 442 – 455, 457 – 476, 478 – 483, 485 – 494, 496 – 683, 685 – 690, 692 – 696, 698 – 1135, 1137, 1139 – 1140, 1142 – 1207, 1209 – 1224, 1226 – 1230, 1232, 1234 – 1238, 1240 – 1243, 1245 – 1286, 1288 – 1342, 1344 – 1454, 1456 – 1459, 1461 – 1468, 1470 – 1594, 1596 – 1598, 1600 – 1604, 1606 – 1625, 1627 – 1648, 1650 – 1657, 1659 – 1759, 1761 – 1784, 1786, 1788 – 1816, 1818 – 1820, 1822 – 1992, 1995 – 2057, 2059 – 2061, 2063, 2065 – 2099, 2101 – 2103, 2105 – 2115, 2117 – 2293, 2295 – 2353, 2355 – 2415, 2417 – 2532, 2534 – 3422, 3424 – 4880, 4882 – 4936, 4938, 4940 – 5007, 5009 – 5045, 5047 – 5056, 5058 – 7554, 7556 – 7570, 7572 – 9047, 9049 – 9081, 9083 – 9161, 9163, 9165 – 10778
House graph H_5	10 662	1 – 3, 5 – 7, 9 – 14, 16 – 34, 36 – 40, 42 – 46, 49 – 52, 54 – 55, 57 – 83, 85 – 278, 280 – 286, 288 – 293, 295 – 312, 314 – 329, 331 – 333, 335 – 340, 342 – 386, 388 – 396, 398 – 401, 403 – 409, 411 – 412, 414 – 423, 425 – 431, 433 – 434, 436 – 440, 442 – 476, 478 – 532, 534 – 537, 539 – 608, 610 – 612, 614 – 643, 646 – 668, 670 – 675, 677 – 873, 875 – 879, 881 – 899, 901 – 934, 936 – 962, 964 – 990, 992 – 993, 995 – 1003, 1005 – 1007, 1009 – 1039, 1041 – 1078, 1080 – 1137, 1139 – 1140, 1142 – 1179, 1181 – 1207, 1209 – 1224, 1226 – 1230, 1232 – 1286, 1288 – 1303, 1305 – 1315, 1317 – 1331, 1333 – 1342, 1345 – 1347, 1349 – 1579, 1581 – 1584, 1586 – 1820, 1822 – 1901, 1903 – 1909, 1911 – 1919, 1921 – 2057, 2059 – 2063, 2065 – 2103, 2105 – 2134, 2136 – 2415, 2417 – 2532, 2534 – 4880, 4882, 4884 – 4921, 4923 – 5056, 5058, 5060 – 5064, 5066 – 6701, 6703, 6705 – 9038, 9041 – 9042, 9044, 9046 – 9992, 9995 – 10747
Kite graph K_5	8 919	1 – 2, 5 – 1352, 1354 – 1356, 1358 – 1361, 1363 – 1367, 1369 – 1374, 1376 – 1381, 1383 – 1396, 1398 – 1399, 1401 – 1418, 1420 – 1442, 1444 – 1445, 1451, 1453 – 1468, 1470 – 1478, 1480, 1482 – 1483, 1487 – 1490, 1492 – 1505, 1507 – 1513, 1516 – 1520, 1522 – 1523, 1525 – 1527, 1530, 1533, 1535 – 1536, 1540 – 1541, 1545 – 1549, 1551 – 1552, 1554 – 1556, 1560 – 1562, 1568 – 1571, 1574 – 1579, 1581, 1583 – 1584, 1586, 1590 – 1592, 1595 – 1784, 1786 – 4926, 4930 – 4935, 4937 – 4938, 4940 – 4948, 4950, 4952 – 4953, 4957 – 4959, 4961, 4967 – 4970, 4972 – 4975, 4979, 4981, 4983, 4985, 4990 – 4993, 4995 – 4997, 4999 – 5002, 5007, 5009 – 5024, 5027 – 5029, 5031 – 5036, 5040, 5042 – 5047, 5049 – 5055, 5058, 5063 – 5064, 5066 – 5070, 5074 – 5077, 5082 – 5083, 5086 – 5087, 5089 – 5090, 5092, 5094 – 5099, 5101, 5103 – 5107, 5109 – 5114, 5116, 5118 – 9047
Ladder graph L_6	9 933	5, 10, 13 – 14, 16 – 17, 20, 22, 26 – 27, 32, 34, 38 – 40, 45, 49, 51, 53 – 55, 57 – 58, 61, 63, 67, 70 – 71, 75 – 78, 80, 83, 86 – 88, 93, 97 – 101, 105 – 115, 118, 121, 123 – 124, 128 – 130, 133 – 137, 139, 142 – 150, 156 – 158, 160, 162 – 177, 181 – 188, 193 – 195, 197, 199 – 200, 202 – 203, 205 – 210, 213 – 227, 229 – 239, 244 – 246, 248, 250 – 254, 256 – 270, 273 – 278, 280, 282 – 283, 285 – 286, 288 – 291, 293, 295 – 296, 298, 300 – 303, 305 – 318, 311 – 315, 317 – 320, 321, 324, 326, 328 – 329, 331 – 332, 335 – 336, 338 – 343, 345 – 347, 349 – 351, 353 – 356, 359, 361, 364, 366 – 370, 372 – 376, 378 – 385, 389 – 390, 392, 396, 398 – 401, 408 – 415, 427, 430, 434, 436 – 438, 440, 442, 444 – 447, 449 – 455, 458 – 459, 464, 466, 469 – 473, 475 – 476, 479 – 480, 482, 485 – 490, 501 – 503, 510, 512 – 514, 517 – 527, 529 – 532, 534 – 544, 550 – 551, 553, 555 – 559, 561 – 683, 686, 688 – 690, 696, 698 – 702, 703 – 714, 716 – 726, 728 – 729, 731 – 733, 735 – 736, 739, 741 – 748, 750 – 753, 756 – 766, 768 – 769, 771 – 777, 779 – 780, 782 – 787, 790 – 821, 825, 828 – 831, 834, 837 – 843, 845 – 862, 864 – 865, 867 – 873, 875 – 901, 903 – 915, 918 – 930, 990 – 992, 994 – 1005, 1008 – 1039, 1042 – 1043, 1045 – 1128, 1130 – 1134, 1135 – 1137, 1139 – 1140, 1142 – 1148, 1150 – 1153, 1155 – 1163, 1165, 1171 – 1181, 1183 – 1185, 1187, 1189 – 1195, 1197 – 1202, 1204 – 1207, 1209 – 1210, 1212 – 1224, 1227 – 1230, 1234 – 1238, 1241 – 1245, 1247 – 1252, 1255, 1257 – 1258, 1260 – 1262, 1264 – 1269, 1271 – 1274, 1276 – 1286, 1288 – 1300, 1310, 1313 – 1315, 1317 – 1319 – 1326, 1338 – 1342, 1344 – 1350, 1352 – 1357, 1360 – 1368, 1370 – 1399, 1402, 1404 – 1405, 1407 – 1412, 1415 – 1454, 1456 – 1457, 1461, 1464, 1466 – 1479, 1481 – 1492, 1494 – 1495, 1498 – 1499, 1502 – 1511, 1513 – 1514, 1516 – 1517, 1519 – 1522, 1524, 1526 – 1539, 1539 – 1546, 1546 – 1547, 1577, 1582 – 1587, 1589, 1592, 1594, 1601, 1604, 1607 – 1608, 1611, 1613 – 1629, 1631, 1641, 1645, 1648, 1652 – 1654, 1659 – 1666, 1662, 1669, 1671 – 1677, 1679 – 1688, 1690 – 1691, 1693 – 1699, 1701 – 1702, 1704, 1716 – 1712, 1715 – 1716, 1718 – 1725, 1727 – 1754, 1756 – 1758, 1759, 1761 – 1762, 1764, 1766 – 1767, 1769, 1771 – 1781, 1784, 1788, 1790 – 1794, 1796, 1799, 1801, 1804, 1806, 1812, 1818, 1822 – 1903, 1907, 1909, 1912, 1914, 1916, 1921 – 1922, 1925 – 1926, 1931, 1935, 1937 – 1944, 1946 – 1947, 1949 – 1950, 1952 – 1954, 1957 – 1977, 1988, 1995 – 2001, 2004, 2006, 2009 – 2012, 2012 – 2014, 2033, 2035 – 2036, 2040 – 2042, 2044, 2046 – 2047, 2050 – 2055, 2063, 2066 – 2072, 2074 – 2077, 2079, 2081 – 2089, 2091 – 2096, 2098 – 2099, 2102 – 2103, 2105 – 2113, 2115, 2117 – 2130, 2132 – 2133, 2136 – 2167, 2169 – 2172, 2174 – 2183, 2186 – 2194, 2196 – 2205, 2208 – 2216, 2218 – 2225, 2254 – 2269, 2273 – 2274, 2276 – 2291, 2293, 2295 – 2306, 2308 – 2310, 2312, 2314 – 2323, 2325 – 2339, 2343 – 2344, 2346 – 2347, 2349, 2351 – 2353, 2355 – 2357, 2359 – 2364, 2366 – 2391, 2393 – 2398, 2399 – 2400 – 2411, 2413 – 2415, 2417 – 2428, 2430 – 2441, 2443 – 2444, 2446 – 2460, 2462 – 2464, 2467 – 2469, 2472 – 2479, 2481 – 2485, 2497 – 2523, 2526 – 2522, 2534 – 2541, 2544 – 2671, 2673 – 2677, 2679 – 2686, 2688 – 2701, 2704 – 2713, 2715 – 2730, 2732, 2736 – 2743, 2745, 2747, 2749 – 2785, 2789 – 2830, 2833 – 2847, 2850, 2852, 2855, 2857 – 3000, 3003 – 3092, 3094, 3102, 3104 – 3105, 3107 – 3159, 3173, 3166, 3168, 3170 – 3171, 3173, 3175, 3177 – 3193, 3195, 3197 – 3271, 3273 – 3285, 3320 – 3342, 3344 – 3346 – 3350, 3352 – 3384, 3384 – 3394, 3398 – 3400, 3403 – 3420, 3422, 3425 – 3426, 3428 – 3576, 3578, 3580 – 3623, 3625 – 3626, 3628 – 3737, 3739 – 3747, 3749 – 3758, 3761 – 3764, 3766 – 3784, 3786 – 3787, 3789 – 3807, 3809 – 3827, 3829, 3831 – 3849, 3851 – 3869, 3871 – 3888, 3890 – 3947, 3949 – 3958, 3961 – 3964, 3967 – 3975, 3977 – 3987, 3989 – 3994, 3996 – 4007, 4009 – 4141, 4144 – 4255, 4257 – 4259, 4267 – 4269 – 4280, 4284 – 4285, 4288 – 4291, 4293 – 4312, 4314 – 4325, 4327, 4329 – 4330, 4332 – 4334, 4336 – 4342, 4344 – 4348, 4348 – 4350, 4355, 4361 – 4362, 4364 – 4368, 4378 – 4388, 4391 – 4393, 4397 – 4403, 4405 – 4409, 4411 – 4414, 4430, 4432, 4434 – 4487, 4489 – 4494, 4495 – 4510, 4496 – 4514, 4514 – 4532, 4534 – 4605, 4607 – 4609, 4611 – 4612, 4615, 4617 – 4621, 4623 – 4648, 4646, 4652 – 4678, 4680 – 4705, 4707 – 4711, 4714 – 4723, 4725 – 4765, 4767 – 4781, 4783 – 4790, 4792, 4794 – 4798, 4800 – 4803, 4805 – 4856, 4858 – 4861, 4863 – 4867, 4869 – 4876, 4878 – 4880, 4882 – 4889, 4891 – 4893, 4895 – 4905, 4908, 4910 – 4912, 4914 – 4918, 4920 – 4926, 4928 – 4936, 4938 – 4940 – 4946, 4948 – 4952, 4954 – 4955, 4957 – 4968, 4970 – 4986, 4988 – 4990 – 4995, 4997, 4999 – 5007, 5011, 5013 – 5015, 5017 – 5027, 5029 – 5045, 5047, 5049 – 5050, 5052 – 5056, 5058, 5060, 5062, 5064 – 5066, 5070 – 5075, 5078, 5080 – 5081, 5083 – 5084, 5086 – 5090, 5092 – 5093, 5095, 5098 – 5101, 5103 – 5108, 5110 – 5111, 5113, 5115 – 5527, 5529 – 5530, 5532 – 5803, 5816 – 6008, 6012, 6014 – 6043, 6046, 6048, 6051 – 6053, 6056 – 6553, 6555 – 6692, 6694 – 6699, 6701, 6703 – 6708, 6711 – 6718, 6720 – 6723, 6725 – 6732, 6734 – 6735, 6737 – 6771, 6773, 6776 – 6785, 6787 – 7018, 7018 – 7022, 7025 – 7140, 7142 – 7198, 7200 – 7273, 7275 – 7278, 7279, 7281, 7283 – 7300, 7304 – 7305, 7307 – 7316, 7318 – 7361, 7363 – 7427, 7430 – 7554, 7557 – 7558, 7560, 7563 – 7581, 7583 – 7585, 7587 – 7897, 7898 – 7900, 8043, 8045 – 8046, 8048 – 8111, 8173 – 8847, 8849 – 8853, 8856 – 8885, 8887 – 8933, 8935 – 8981, 8983 – 8985, 8987 – 9039, 9041 – 9042, 9044 – 9047, 9050, 9054 – 9081, 9083 – 9161, 9166 – 9170, 9172 – 9239, 9242 – 9243, 9245 – 9277, 9279 – 9925, 9927 – 10145, 10147 – 10778

TABLE III. Complete list of 4-regular graphs on 13 vertices sharing the considered induced subgraphs.